

## Big Bang nucleosynthesis and tensor-scalar gravity

Thibault Damour

*Institut des Hautes Etudes Scientifiques, 91440 Bures-sur-Yvette, France  
and*

*DARC, CNRS-Observatoire de Paris, 92195 Meudon, France*

Bernard Pichon

*DARC, CNRS-Observatoire de Paris, 92195 Meudon, France*

### Abstract

Big Bang Nucleosynthesis (BBN) is studied within the framework of a two-parameter family of tensor-scalar theories of gravitation, with nonlinear scalar-matter coupling function  $a(\varphi) = a_0 + \alpha_0(\varphi - \varphi_0) + \frac{1}{2}\beta(\varphi - \varphi_0)^2$ . We run a BBN code modified by tensor-scalar gravity, and impose that the theoretically predicted BBN yields of Deuterium, Helium and Lithium lie within some conservative observational ranges. It is found that large initial values of  $a(\varphi)$  (corresponding to cosmological expansion rates, for temperatures higher than 1 MeV, much larger than standard) are compatible with observed BBN yields. However, the BBN-inferred upper bound on the cosmological baryon density is insignificantly modified by considering tensor-scalar gravity. Taking into account the effect of  $e^+e^-$  annihilation together with the subsequent effect of the matter-dominated era (which both tend to decouple  $\varphi$  from matter), we find that the present value of the scalar coupling, i.e. the present level of deviation from Einstein's theory, must be, for compatibility with BBN, smaller than  $\alpha_0^2 \lesssim 10^{-6.5} \beta^{-1} (\Omega_{\text{matter}} h^2 / 0.15)^{-3/2}$  when  $\beta \gtrsim 0.5$ .

## I. INTRODUCTION

The idea that Einstein’s tensor gravitational field might be accompanied by a massless scalar partner was first suggested in the twenties by Kaluza [1]. Since then, such tensor-scalar gravity theories have been studied in detail by many authors [2–7]. String theory has recently revived the motivation for considering gravitational-strength scalar fields, such as the (model-independent) dilaton or the (Kaluza-Klein-type) moduli (see, e.g., [8]). In the simplest versions of tensor-scalar theories of gravity (those respecting the equivalence principle) the coupling between matter and the scalar field  $\varphi$  is described by a single “coupling function”  $a(\varphi)$ , such that all physical mass scales get multiplied by a factor  $A(\varphi) \equiv \exp[a(\varphi)]$  when measured in “Einstein units” (see below for the definition of the Einstein conformal frame). For instance, the Jordan-Fierz-Brans-Dicke (JFBD) theory is the one-parameter theory defined by a linear coupling function,  $a(\varphi) = \alpha_0 \varphi$ . The JFBD theory is not an appealing alternative to general relativity because its only (dimensionless) parameter  $\alpha_0$  needs to be fine-tuned to a small value,  $\alpha_0^2 < 10^{-3}$ , to be consistent with existing experimental data. [See, e.g., [9] for a discussion of the constraints on tensor-scalar gravity brought by solar-system, and binary pulsar, data.] By contrast, it has been shown that more general theories with nonlinear coupling functions, containing no small parameters, can be naturally compatible with experimental data because the cosmological evolution drives the background value of  $\varphi$  toward a value that minimizes the coupling function  $a(\varphi)$ , thereby reducing by a large factor all the present observable effects of  $\varphi$  [10], [11]. Within such cosmological-attractor models, the only regime in which the scalar field can play a quantitatively important role is early cosmology.

Big Bang nucleosynthesis (BBN) is the earliest cosmological process that is physically well established and about which one has reasonably accurate observational data. Its importance for constraining many physical or astrophysical scenarios was first pointed out by Shvartsman [12]. For recent treatments see, e.g., [13–15]. In particular, BBN is crucially used for deriving an upper bound on the cosmological baryon density  $\Omega_b = \rho_{\text{baryon}}/\rho_{\text{closure}}$  which, even for extreme parameters, is claimed to be  $\Omega_b < 0.03 h^{-2} < 0.2$  [13–15] (here,  $h \equiv H_0/(100 \text{ km s}^{-1} \text{ Mpc}^{-1})$ ). One of the main motivations of the present paper is to examine whether the presence of a gravitational-strength scalar field  $\varphi$ , having a generic non-JFBD, i.e., nonlinear, coupling function  $a(\varphi)$ , can significantly modify the standard limit on  $\Omega_b$ , while being still compatible with present gravitational experiments. A secondary motivation is to study the level of present scalar admixture to Einstein’s gravity (observable, in principle, in precision tests of relativistic gravity) which is naturally compatible with BBN data, i.e. with observed light element abundances.

Our analysis is more general and/or more exact than previous attacks on this problem. Indeed, we consider the case of a nonlinear coupling function  $a(\varphi)$  admitting a local minimum, while most previous studies restricted themselves to JFBD-type theories [16–18] (see also the related studies of BBN limits on the variability of the gravitational constant  $G$  [12], [19–22]). A recent work by Santiago et al. [23] has considered nonlinear coupling functions  $a(\varphi)$  of the type we shall study but their analysis is, in our opinion, less satisfactory than

ours in two<sup>1</sup> ways: (i) they approximated the effect of  $\varphi$  as a *small, constant speed up factor*  $\xi_n$  affecting only the value of the neutron/proton ratio at some effective “freeze-out”, supposed to take place before and separately from  $e^+e^-$  annihilation, without recomputing in tensor-scalar gravity the production of all the light elements, and (ii) they related the value of  $\varphi$  (and the corresponding  $\xi_n$ ) at freeze-out to its present value  $\varphi_0$  by *integrating backward in time*. Concerning the point i), we shall, instead, find that the beginning of  $e^+e^-$  annihilation generates a source term for the evolution of  $\varphi$  which generically (especially for largish values of  $\beta$ ) cannot be neglected during freeze-out so that the speed up factor can vary a lot during the critical freezing of the  $n/p$  ratio. ( see Section 4 for a more detailed discussion). Concerning ii), the procedure of backward time-integration may generically lead to incorrect results because the  $\varphi$  evolution equation is similar to that of a damped harmonic oscillator [10]. Integrating backward in time such an equation is equivalent to integrating forward in time an oscillator with negative friction, which introduces spurious runaway solutions. The origin of the introduction of these runaway solutions is simply that, when integrating backward in time, one lacks the correct “initial” condition for the present time derivative of  $\varphi$ ,  $\dot{\varphi}_0$ , corresponding to some  $\varphi_0$ . [Indeed,  $\dot{\varphi}_0$  is nonlocally defined by the full forward (damped) evolution of  $\varphi$  starting from the physically natural initial condition,  $\dot{\varphi}_{\text{in}} = 0$ , deep into the radiation era (see below).] We suppose that this pollution by runaway solutions is the root of the (incorrect) obtention of infinite peaks in the figures of Ref. [23], corresponding to speed-up factors equal to one (which is physically forbidden, as we shall discuss below). [We also suppose that this pollution by runaway solutions, made more critical because of a direct numerical integration from the present time back to BBN time, invalidates the physical relevance of the work of Ref. [24], and explains why their limits on the coupling parameter  $\alpha_0^2$  are about fourteen orders of magnitude smaller than the limits we get here.] However, we have not checked our supposition (concerning the effect of runaway solutions) by running reverse integrations ourselves.

In this work, we shall avoid this potential problem of unphysical runaway solutions by integrating only forward in time. Another difference with previous work is that we shall compute, using a full BBN code modified by tensor-scalar gravity effects, the abundances of all the light elements: Deuterium, Helium 3, Helium 4 and Lithium 7. Indeed, though they are still large uncertainties on the primordial abundances of these elements, it is important to combine the predicted abundances of all the light elements with the corresponding observational bounds to get consistent constraints on tensor-scalar gravity.

The present paper works within the framework defined by the following assumptions: (i) we consider tensor-scalar gravitation theories containing a single massless scalar field  $\varphi$ , (ii) the coupling function of  $\varphi$  is restricted to the two-parameter family  $a(\varphi) = a_0 + \alpha_0(\varphi - \varphi_0) + \frac{1}{2}\beta(\varphi - \varphi_0)^2$  (see Section II for the choice of this quadratic form), (iii) we require that deep into the radiation era the time derivative of  $\varphi$  vanishes (see our detailed discussion below), and (iv) we consider the case of a spatially flat Friedmann universe (the effect of non zero curvature has been investigated in Ref. [10]).

---

<sup>1</sup>In addition, the solution for  $\varphi$  during the end of the radiation-dominated epoch is incorrectly given in Sec. IV D of Ref. [23]: e.g., their Eq. (4.37) should contain  $J_1(x)/x$  and  $Y_1(x)/x$ .

## II. TENSOR-SCALAR GRAVITY THEORIES

We consider tensor-scalar gravitation theories containing a single (massless) scalar field, assumed to couple to the trace of the energy-momentum tensor. This coupling means that the scalar source is (for bodies having negligible self gravity) proportional to the (inertial) mass, so that the equivalence principle is respected. The most general theory describing such a mass-coupled long-range scalar field contains one arbitrary coupling function [3]

$$A(\varphi) \equiv \exp(a(\varphi)). \quad (2.1)$$

The action defining the theory reads

$$S = \frac{1}{16\pi G_*} \int d^4x g_*^{1/2} (R_* - 2g_*^{\mu\nu} \partial_\mu \varphi \partial_\nu \varphi) + S_m[\psi_m; A^2(\varphi)g_{\mu\nu}^*]. \quad (2.2)$$

Here,  $G_*$  denotes a bare gravitational coupling constant,  $R_* \equiv g_*^{\mu\nu} R_{\mu\nu}^*$  the curvature scalar of the ‘‘Einstein metric’’  $g_{\mu\nu}^*$  describing the pure spin-2 excitations, and  $\varphi$  the long-range scalar field describing spin-0 excitations. [We use the signature  $-+++$  and the notation  $g_* \equiv -\det g_{\mu\nu}^*$ .] The last term in Eq. (2.2) denotes the action of matter, which is a functional of some matter variables (collectively denoted by  $\psi_m$ ) and of the (Jordan-Fierz) ‘‘physical metric’’

$$\tilde{g}_{\mu\nu} \equiv A^2(\varphi) g_{\mu\nu}^*. \quad (2.3)$$

Laboratory clocks and rods measure the metric  $\tilde{g}_{\mu\nu}$  which, in the model considered here, is universally coupled to matter. In the BBN context, the standard laws of nongravitational physics (such as nuclear reaction rates and thermodynamical laws) will hold in their usual form when expressed in ‘‘physical units’’, i.e. in units of the proper interval  $d\tilde{s}^2 = \tilde{g}_{\mu\nu} dx^\mu dx^\nu$ . For instance, Noether’s theorem applied to the matter action  $S_m[\psi_m; \tilde{g}_{\mu\nu}]$  yields the usual law of conservation of energy and momentum:

$$\tilde{\nabla}_\nu \tilde{T}^{\mu\nu} = 0, \quad (2.4)$$

where  $\tilde{T}^{\mu\nu} \equiv 2\tilde{g}^{-1/2} \delta S_m / \delta \tilde{g}_{\mu\nu}$  is the material stress-energy tensor in physical units. In Eq. (2.4) the covariant derivative  $\tilde{\nabla}_\nu$  is that defined by  $\tilde{g}_{\mu\nu}$ .

On the other hand, the gravitational field equations of the theory are most simply formulated in terms of the pure-spin variables  $(g_{\mu\nu}^*, \varphi)$ . From (2.2), they read

$$R_{\mu\nu}^* = 2\partial_\mu \varphi \partial_\nu \varphi + 8\pi G_* \left( T_{\mu\nu}^* - \frac{1}{2} T^* g_{\mu\nu}^* \right), \quad (2.5a)$$

$$\square_{g^*} \varphi = -4\pi G_* \alpha(\varphi) T^*, \quad (2.5b)$$

with  $T_*^{\mu\nu} \equiv 2g_*^{-1/2} \delta S_m / \delta g_{\mu\nu}^*$  denoting the material stress-energy tensor in Einstein units. It is related to the physical-units stress-energy tensor through

$$g_{\nu\sigma}^* T_*^{\mu\sigma} \equiv T_{*\nu}^\mu = A^4(\varphi) \tilde{T}_\nu^\mu \equiv A^4(\varphi) \tilde{g}_{\nu\sigma} \tilde{T}^{\mu\sigma}. \quad (2.6)$$

The quantity  $\alpha(\varphi)$  on the R.H.S. of Eq. (2.5b) plays a crucial role in the theory. It is the logarithmic derivative of the coupling function,

$$\alpha(\varphi) \equiv \frac{\partial \ln A(\varphi)}{\partial \varphi} \equiv \frac{\partial a(\varphi)}{\partial \varphi}, \quad (2.7)$$

and it measures the basic (field-dependent) coupling strength between the scalar field and matter. The JFBD theory is defined by a linear field dependence of  $a(\varphi) = \ln A(\varphi) = \alpha_0 \varphi$ , i.e. by a constant (field-independent) coupling strength  $\alpha(\varphi) = \alpha_0$  [ $\alpha_0^2 = (2\omega + 3)^{-1}$  in the notation of [4]]. Generically, one might expect a nonlinear field dependence of  $a(\varphi)$  leading to a field-dependent coupling strength  $\alpha(\varphi)$ . It has been shown in Refs. [7], [25] that all *weak field* (“post-Newtonian”) deviations from general relativity (of any post-Newtonian order) can be expressed in terms of the values of  $\alpha(\varphi)$  and of its successive  $\varphi$ -derivatives, starting with

$$\beta(\varphi) \equiv \frac{\partial \alpha(\varphi)}{\partial \varphi}, \quad (2.8)$$

at the present “vacuum expectation value”  $\varphi_0$  of the field  $\varphi$ . Here  $\varphi_0$  denotes the asymptotic value of  $\varphi$  at spatial infinity, at the present epoch. At the first post-Newtonian approximation, deviations from general relativity are proportional to the well-known Eddington-Nordtvedt-Will parameters

$$\bar{\gamma} \equiv \gamma_{\text{Edd}} - 1 = -2 \alpha_0^2 / (1 + \alpha_0^2), \quad (2.9a)$$

$$\bar{\beta} \equiv \beta_{\text{Edd}} - 1 = +\frac{1}{2} \beta_0 \alpha_0^2 / (1 + \alpha_0^2)^2, \quad (2.9b)$$

where  $\alpha_0 \equiv \alpha(\varphi_0)$  and  $\beta_0 \equiv \beta(\varphi_0)$ . We see explicitly from Eqs. (2.9) that post-Newtonian deviations from general relativity tend to zero with  $\alpha_0$  at least as fast as  $\alpha_0^2$ . This holds true for *weak-field* deviations of arbitrary post-Newtonian order [25]. By contrast, it was found in Ref. [26] that *strong-field* deviations from general relativity do not tend to zero with  $\alpha_0$  if the parameter  $\beta_0 \equiv \beta(\varphi_0) \equiv \partial \alpha(\varphi_0) / \partial \varphi_0$  is sufficiently negative. However, if one considers (as we shall do here) the case where the cosmological-attractor mechanism of Refs. [10], [11] takes place, the parameter  $\beta_0$  is necessarily positive. Indeed, Refs. [10], [11] found that the spatial average of  $\varphi$  is attracted, during the cosmological evolution, toward a *minimum* of the coupling function  $a(\varphi)$ . Therefore, the present cosmological value of  $\varphi$ ,  $\varphi_0 = \varphi(t_0)$ , is generically expected to be very close to a value  $\varphi_m$  such that  $\alpha_m = \partial a(\varphi_m) / \partial \varphi_m = 0$  and  $\beta_m = \partial^2 a(\varphi_m) / \partial \varphi_m^2 > 0$ . In such a case, all present deviations from general relativity (weak-field ones and strong-field ones alike) are expected to be very small, because they all contain a factor  $\alpha_0^2 \simeq [\beta_m(\varphi_0 - \varphi_m)]^2 \ll 1$ .

As was discussed in Refs. [10], [11], and is recalled in Section 3 below, the Einstein-time evolution for  $\varphi$  deep into the radiation dominated era can be approximated by  $\ddot{\varphi} + 3H_* \dot{\varphi} \simeq 0$ , which shows that  $\dot{\varphi}$  decreases, during the expansion, as the inverse cube of the Einstein-frame scale factor  $R_*$  (in usual cosmological parlance, one can say that  $\dot{\varphi}$  contains only a decreasing mode). Therefore the natural initial conditions for  $\varphi$  deep into the radiation era are that  $\dot{\varphi}$  vanishes, while  $\varphi = \varphi_{\text{in}}$  has an arbitrary value. Starting from these values,  $\varphi$  will run *down* the coupling function  $a(\varphi)$  and will be attracted to the *nearest* minimum of  $a(\varphi)$ . [Note that this shows, as emphasized in Ref. [10], that the value of  $a(\varphi)$  irreversibly decreases during the expansion, so that the speed up factor must always be larger than one.] As the generic behaviour of a function near a minimum is parabolic,  $a(\varphi) = a(\varphi_m) + \frac{1}{2} \beta_m (\varphi - \varphi_m)^2 +$

$\mathcal{O}((\varphi - \varphi_m)^3)$ , it is plausible to assume that  $a(\varphi)$  is roughly parabolic in the whole interval around  $\varphi_m$  containing  $\varphi_{\text{in}}$ . We shall therefore follow Ref. [9] and study the paradigmatic case where the coupling function is quadratic in  $\varphi$ ,  $a_{\text{quad}}(\varphi) = a_0 + \alpha_0(\varphi - \varphi_0) + \frac{1}{2}\beta_0(\varphi - \varphi_0)^2$ . This case is the simplest generalization of the JFBD theory ( $a_{\text{JFBD}}(\varphi) = a_0 + \alpha_0(\varphi - \varphi_0)$ ) admitting a nonlinear coupling function, and susceptible of being cosmologically attracted to a point where  $\varphi$  decouples from matter. By appropriately choosing the unit of length one can fix  $a_0$  to zero. One can also conventionally fix the minimum of  $a(\varphi)$  at  $\varphi_m \equiv 0$ . Therefore, without loss of generality, we shall write the general “quadratic model” in the simple form

$$a_{\text{quad}}(\varphi) \equiv \ln A_{\text{quad}}(\varphi) = \frac{1}{2}\beta\varphi^2, \quad (2.10)$$

with  $\beta > 0$ . This model contains two free parameters: the quantity  $\beta = \partial^2 a(\varphi)/\partial\varphi^2$  ( $= \beta_0 = \beta_m$ ), and, either the initial value  $\varphi_{\text{in}}$  of  $\varphi$  deep in the radiation dominated era, or, alternatively, the present value  $\varphi_0$  of  $\varphi$ . The aim of the present paper is to investigate which values of  $\beta$  and  $\varphi_{\text{in}}$  (and consequently,  $\varphi_0$ ) are compatible with BBN data.

### III. BIG BANG NUCLEOSYNTHESIS IN TENSOR-SCALAR GRAVITY

As mentioned in Section 2, the standard laws of nongravitational physics will keep their usual form if one measures lengths and times in “physical units”, i.e. in units of the interval  $d\tilde{s}^2 = \tilde{g}_{\mu\nu} dx^\mu dx^\nu = A^2(\varphi) ds_*^2$ . In a cosmological context, the physical interval will read

$$d\tilde{s}^2 = -d\tilde{t}^2 + \tilde{R}^2(\tilde{t}) d\ell^2, \quad (3.1)$$

where  $\tilde{t}$  is the physical cosmological time, and  $\tilde{R}$  the physical scale factor. Here

$$d\ell^2 = \frac{dr^2}{1 - kr^2} + r^2(d\theta^2 + \sin^2\theta d\phi^2), \quad (3.2)$$

is the metric of a 3-space of constant curvature  $k = +1, 0$  or  $-1$ . The corresponding physical expansion rate (Hubble parameter) is

$$\tilde{H} = \frac{d}{d\tilde{t}} \ln \tilde{R}. \quad (3.3)$$

The Einstein-frame counterparts of the above quantities are

$$ds_*^2 = -dt_*^2 + R_*^2(t_*) d\ell^2, \quad (3.4)$$

$$H_* = \frac{d}{dt_*} \ln R_*. \quad (3.5)$$

The relation  $d\tilde{s}^2 = A^2(\varphi) ds_*^2$  gives the links

$$d\tilde{t} = A(\varphi) dt_*, \quad (3.6a)$$

$$\tilde{R} = A(\varphi) R_*. \quad (3.6b)$$

Let us introduce the notation  $\chi$  for the Einstein-time derivative of  $\varphi$ :

$$\chi \equiv \frac{d\varphi}{dt_*} \equiv A(\varphi) \frac{d\varphi}{dt}. \quad (3.7)$$

In terms of this notation, the links (3.6) give the following relation between the Hubble parameters,

$$\widetilde{H} = (A(\varphi))^{-1} [H_* + \alpha(\varphi) \chi], \quad (3.8)$$

where  $\alpha(\varphi) \equiv \partial a(\varphi)/\partial \varphi$ .

We computed BBN by using Kawano's update [27] of Wagoner's code [28]. This code evolves thermodynamical variables and nuclear abundances as functions of the physical temperature  $\widetilde{T}$ . All these physical evolution equations are unchanged in tensor-scalar gravity. The only modifications that need to be brought to this code are: (i) a modified expression for the physical expansion rate  $\widetilde{H}$  as a function of the energy density, and (ii) two new first-order equations giving the evolution of the scalar field. Note that we assume three light neutrinos throughout this work.

To get the modified expression for the expansion rate we need to write explicitly the modified Einstein equations (2.5a). In the present cosmological context they yield

$$-\frac{3}{R_*} \frac{d^2 R_*}{dt_*^2} = 4\pi G_* (\rho_* + 3p_*) + 2\chi^2, \quad (3.9a)$$

$$3H_*^2 + 3\frac{k}{R_*^2} = 8\pi G_* \rho_* + \chi^2. \quad (3.9b)$$

Here  $\rho_*$  and  $p_*$  are the Einstein-units energy density and pressure, linked to their physical counterparts by Eq. (2.6), i.e. by

$$\rho_* = A^4 \widetilde{\rho}, \quad p_* = A^4 \widetilde{p}, \quad (3.10)$$

where  $A \equiv A(\varphi)$ . As usual, the curvature term  $k/R_*^2$  in Eq. (3.9b) is negligible during BBN so that Eq. (3.9b) gives the following result for  $H_*$  in terms of the physical energy density and  $\chi \equiv d\varphi/dt_*$

$$H_* = \sqrt{\frac{8\pi G_*}{3} A^4 \widetilde{\rho} + \frac{1}{3} \chi^2}. \quad (3.11)$$

The corresponding physical Hubble parameter is then computed by using Eq. (3.8).

It remains to write explicit evolution equations for the scalar field  $\varphi$ . Eq. (2.5b) yields

$$\frac{d^2 \varphi}{dt_*^2} + 3H_* \frac{d\varphi}{dt_*} = -4\pi G_* \alpha(\varphi) (\rho_* - 3p_*). \quad (3.12)$$

In terms of the variable  $\chi$ , Eq. (3.7), and of the physical time  $\widetilde{t}$ , this gives the first-order system

$$\frac{d\varphi}{d\tilde{t}} = A^{-1} \chi, \quad (3.13a)$$

$$\frac{d\chi}{d\tilde{t}} = -A^{-1} [3 H_* \chi + 4\pi G_* \alpha(\varphi) A^4 \tilde{\sigma}], \quad (3.13b)$$

where  $\tilde{\sigma}$  denotes the following “source term”

$$\tilde{\sigma} = \tilde{\rho} - 3\tilde{p}. \quad (3.14)$$

Around the period of primordial nucleosynthesis, the scalar source term can be approximated by

$$\tilde{\sigma}_{\text{BBN}} \simeq \tilde{\sigma}_e \equiv \tilde{\rho}_e - 3\tilde{p}_e, \quad (3.15)$$

where the index “ $e$ ” denotes the contribution from electrons and positrons. Indeed, among the various contributions to the total energy entering Eq. (3.11),

$$\tilde{\rho} = \tilde{\rho}_\gamma + \tilde{\rho}_e + \tilde{\rho}_\nu + \tilde{\rho}_m, \quad (3.16)$$

the massless (or, at least, ultrarelativistic) photon and neutrino contributions  $\tilde{\rho}_\gamma$ ,  $\tilde{\rho}_\nu$  satisfy  $\tilde{\sigma}_\gamma = 0 = \tilde{\sigma}_\nu$ , while the non relativistic matter contribution  $\tilde{\rho}_m$  (cold dark matter plus baryons) is negligibly small (it becomes, however, important later, around matter-radiation equivalence and during the matter dominated era). By contrast, it happens by coincidence that one of the most important phenomena of BBN, the freezing out of the neutron to proton ratio, takes place around a physical temperature  $\tilde{T}_F \sim 1$  MeV, which is precisely when the  $e^+ e^-$  plasma starts becoming non relativistic before annihilating. In other words, the freeze-out of  $(n/p)$  takes place when there is a numerically large contribution  $\tilde{\sigma}_e$  to the source driving the evolution of the scalar field  $\varphi$ . This fact has been taken into account only in the coarse approximation of considering that the freeze-out takes place before, and separately from,  $e^+ e^-$  annihilation in Ref. [23]. Our full numerical integration of a scalar-tensor BBN code shows that  $\tilde{\sigma}_e$  drives a strong (generically oscillatory) evolution of  $\varphi$  at the same time (if not before) the  $(n/p)$  ratio freezes out (See Section IV C below).

Summarizing, we completed an existing standard BBN code [28], [27] by adding: (i) Eqs. (3.8), (3.11) for computing  $\tilde{H}$  in terms of  $\tilde{\rho}$ ,  $\varphi$  and  $\chi$ , and (ii) Eqs. (3.13) for computing the  $\tilde{t}$ -evolution of  $\varphi$  and  $\chi$ . The source terms in these additional equations were taken to be (3.15) and (3.16). We used for the crucial scalar source  $\tilde{\sigma}_e$  the expansion

$$\tilde{\sigma}_e = \frac{2}{\pi^2} \tilde{m}_e^4 \sum_{n=1}^{\infty} (-)^{n+1} \frac{K_1(nz)}{nz}. \quad (3.17)$$

Here,  $K_1$  is a modified Bessel function, and  $z \equiv \tilde{m}_e/\tilde{T}$  (in units where  $\hbar = c = k = 1$ ). As this is an alternating series, it is numerically important to retain an *even* (and large enough) number of terms. We kept sixteen terms in the expansion (3.17). [By contrast, Kawano’s code uses five terms. Note also that the coefficient in front of this expansion is misprinted<sup>2</sup> in Ref. [23].] See Eq. (3.23) below for the exact, unexpanded expression of  $\tilde{\sigma}_e$ .

---

<sup>2</sup> We were informed by the authors of Ref. [23], that they used the correct value in their code.



The rest of the code computes the evolution of thermodynamical variables and of nuclear abundances in terms of the physical temperature  $\tilde{T}$ . The link between physical temperature  $\tilde{T}$  and physical time  $\tilde{t}$  is given by the standard thermodynamical relation

$$\frac{d\tilde{T}}{d\tilde{t}} = -3 \frac{\tilde{\rho} + \tilde{p}}{d\tilde{\rho}/d\tilde{T}} \tilde{H}. \quad (3.18)$$

The input data for each run of the code are:

$$\eta = (4/11) (\tilde{n}_b/\tilde{n}_\gamma)_{\text{in}}, \quad \varphi_{\text{in}}, \quad \chi_{\text{in}} \quad \text{and} \quad \beta. \quad (3.19)$$

The coefficient 4/11 is introduced so that  $\eta$  measures the final baryon-to-photon ratio,  $\eta = (\tilde{n}_b/\tilde{n}_\gamma)_{\text{out}}$ , obtained after  $e^+e^-$  annihilation. As is discussed below, when  $\beta$  is larger than about 0.2, the bare Newton constant  $G_*$  entering Eqs. (3.11) and (3.13b) can be taken to be numerically equal to the value presently measured in Cavendish experiments,  $G_* \simeq 6.672 \times 10^{-8} \text{ cm}^3 \text{ g}^{-1} \text{ s}^{-2}$ . [This is because the cosmological attraction of  $\varphi$  toward  $\varphi_m = 0$  is quite efficient when  $\beta \geq 0.2$ , so that the presently observable value  $\tilde{G}(\varphi_0) = G_* A^2(\varphi_0) [1 + \alpha^2(\varphi_0)]$  differs negligibly from  $G_*$ .] The output data for each run are then<sup>3</sup>

$$\varphi_{\text{out}}, \quad \text{D/H}, \quad {}^3\text{He/H}, \quad Y({}^4\text{He}) \quad \text{and} \quad {}^7\text{Li/H}. \quad (3.20)$$

The ratio  $\text{D/H} \equiv n(\text{D})/n(\text{H})$  denotes, for instance, the number of Deuterium nuclei per proton after BBN, while  $Y({}^4\text{He}) \simeq 4n({}^4\text{He})/(n(\text{H}) + 4n({}^4\text{He}))$  is the abundance by weight of Helium 4. The other physical parameters needed in the code are taken to have their currently measured values (in physical units). In particular, the neutron (exponential) lifetime is taken to be  $\tau_n = 888.54 \text{ s}$ .

An important issue (which, in our opinion, was not properly dealt with in previous work) concerns the initial values for  $\varphi$  and its derivative  $\chi = d\varphi/dt_*$ . Our numerical calculations integrate the evolution for  $\varphi$  in the normal direction, i.e. forward in time. If we insert our paradigmatic quadratic coupling function (2.10), leading to the simple linear coupling strength

$$\alpha_{\text{quad}}(\varphi) = \beta \varphi, \quad (3.21)$$

into Eq. (3.12), we see that  $\varphi(t_*)$  satisfies the equation (here  $\dot{\varphi} \equiv d\varphi/dt_*$ ,  $\sigma_* \equiv \rho_* - 3p_*$ )

$$\ddot{\varphi} + 3H_* \dot{\varphi} + 4\pi G_* \sigma_* \beta \varphi = 0. \quad (3.22)$$

This is the equation of a *damped* harmonic oscillator with time-varying *positive friction*  $f = 3H_*$ , and time-varying positive spring constant  $\omega_0^2(t_*) \equiv 4\pi \beta G_* \sigma_*$ . Indeed, the scalar source  $\sigma_* = \rho_* - 3p_* = A^4(\tilde{\rho} - 3\tilde{p})$  is always positive for a thermal distribution of particles [10], [11],

$$\tilde{\rho}_A - 3\tilde{p}_A = \frac{g_A \tilde{m}_A^2}{2\pi^2} \int_0^\infty \frac{dq q^2}{\tilde{E}_A [\exp(\tilde{E}_A/\tilde{T}) \pm 1]}, \quad \tilde{E}_A = \sqrt{\tilde{m}_A^2 + q^2}. \quad (3.23)$$

---

<sup>3</sup>We do not mention  ${}^7\text{Be}$  and  ${}^8\text{Li}$  which we shall not use.

Here,  $\tilde{m}_A$  is the mass of the considered particle,  $g_A$  is its number of degrees of freedom, and the upper (lower) sign holds for Fermions (Bosons). As emphasized in Refs. [10], [11] the positive damping in Eq. (3.22) means that when one starts the  $\varphi$  evolution very early in the radiation-dominated era (where the total number of effective relativistic degrees of freedom is large) and/or for temperatures well away from any mass threshold  $\tilde{T} \neq \tilde{m}_A$  (so that the “spring constant” term is relatively negligible in Eq. (3.22)) any initial “velocity”  $\dot{\varphi}_{\text{in}} = \chi_{\text{in}}$  (satisfying  $\chi_{\text{in}} \leq \sqrt{3}H_{*\text{in}}$  from Eq. (3.9b) with  $k = 0$ ) will be generically quickly (in a few  $e$ -folds) damped away (as said above, in these circumstances,  $\dot{\varphi}$  decreases like  $R_*^{-3}$ ). Therefore, a physically most natural requirement is to impose (as we do in this work) that the initial velocity  $\chi_{\text{in}}$  *vanish* when starting a BBN run at a temperature  $\tilde{m}_\mu \gg \tilde{T} \gg \tilde{m}_e$ . [The physical effects due to  $\varphi$  would be stable under using only an inequality  $\chi_{\text{in}} \ll H_*$ , instead of a strict vanishing of  $\chi_{\text{in}}$ .] Evidently, there exist mathematical solutions to Eq. (3.22) where  $\dot{\varphi}/H_*$  is not small before BBN. In view of the argument presented above, and in absence of a generic mechanism giving rise to large (i.e. very near  $\sqrt{3}$ ) initial values of  $\dot{\varphi}/H_*$ , we think that such solutions are physically irrelevant.

On the other hand, the initial “position”  $\varphi_{\text{in}}$  is physically unrestricted, at least if the curvature parameter  $\beta$  is not very much larger than unity. [It was shown in Refs. [10], [11] that when  $\beta > 10$ , the effect of the previous mass thresholds (above the electron one) is very efficient in attracting  $\varphi$  toward zero, so that in this case one would expect  $\varphi_{\text{in}}$  before BBN to be small.] In this work, we shall formally leave  $\varphi_{\text{in}}$  unrestricted, even when  $\beta \sim 100$ , to see what constraints BBN brings on this possibility. As the explicit numerical calculations we made start at the temperature  $\tilde{T}_0 = 10^{11} K \sim 10 \text{ MeV}$  which is only 20 times larger than  $\tilde{m}_e$ , we have slightly refined the initial conditions by taking into account the attracting effect of the source term  $\sigma_*$  in Eq. (3.22), integrated over the temperatures  $\tilde{m}_\mu > \tilde{T} \gg \tilde{T}_0$ . Using the asymptotic behaviour  $\tilde{\sigma}_e \propto \tilde{T}^{-2}$  as  $\tilde{T} \gg \tilde{m}_e$ , one finds that, starting from  $\varphi = \varphi_{\text{in}}$ ,  $\chi = \chi_{\text{in}} = 0$  at  $\tilde{m}_\mu > \tilde{T} \gg \tilde{T}_0 \gg \tilde{m}_e$ , one ends up with the following corrected initial conditions at  $\tilde{T} = \tilde{T}_0$ :

$$\varphi(\tilde{T}_0) \simeq \varphi_{\text{in}} - \frac{1}{4} \alpha_{\text{in}} \left( \frac{\tilde{\sigma}}{\tilde{\rho}} \right)_{\tilde{T}_0}, \quad (3.24a)$$

$$\chi(\tilde{T}_0) \simeq -\frac{1}{2} H_* \alpha_{\text{in}} \left( \frac{\tilde{\sigma}}{\tilde{\rho}} \right)_{\tilde{T}_0}, \quad (3.24b)$$

where  $\alpha_{\text{in}} = \alpha(\varphi_{\text{in}})$ . This “edge correction” refinement had, anyway, a negligible effect on our results. The important point to remember of this discussion is that the forward integration in time leads to a physically straightforward, and well motivated, choice for the initial time-derivative of  $\varphi$ . By contrast, any integration backward in time is equivalent to integrating an oscillator with *negative friction* (time-reverse of (3.22), with  $\bar{f} = -f = -3H_*$ ). Such an integration is unstable and may generically lead to including (without knowing it) a “runaway” mode in  $\varphi$ , i.e. a spurious backward-growing mode (equivalent to setting a large, non zero value of  $\chi_{\text{in}}$  at  $\tilde{T} \gg \tilde{m}_e$ ). We think that this incorrect inclusion of spurious runaway modes affects the methods used in Refs. [23] and [24], and may have invalidated some of their results.

## IV. RESULTS OF NUMERICAL INTEGRATIONS AND THEIR COMPARISON WITH OBSERVATIONAL DATA

### A. Primordial abundances: observations

The uncertainties in the “observed” primordial abundances of the light elements (Deuterium, Helium 3, Helium 4, Lithium 7, ...) are large and fraught with systematic errors which are difficult to assess. See Refs. [13], [14] for recent overviews of the observational situation. As the aim of the present paper is to set conservative limits on possible deviations from the “standard” (Einstein-gravity) BBN we wish to work with the most extreme (hopefully “ $3\sigma$ ”-type) ranges for the possible “observed” primordial abundances. We shall take

$$0.21 < Y(^4\text{He}) < 0.255, \tag{4.1a}$$

$$1.5 \times 10^{-5} < \text{D}/\text{H} < 2.4 \times 10^{-4}, \tag{4.1b}$$

$$0.7 \times 10^{-10} < {}^7\text{Li}/\text{H} < 1 \times 10^{-9}. \tag{4.1c}$$

Let us comment briefly on our choices. The minimum value  $Y_{\min} = 0.21$  of Eq. (4.1a) is the one admitted (as extreme possibility) by Refs. [13] and [14], while  $Y_{\max} = 0.255$  is an extreme maximum value suggested by Ref. [29]. The minimum value for D/H, Eq. (4.1b), is from [14], while the maximum one was derived by assuming that the “high” Deuterium value (with its one-sigma error bar) reported by Ref. [30] might be correct. We are aware of the observational results, and arguments, of Tytler and collaborators converging toward a “low” Deuterium value, say [31],

$$\text{D}/\text{H} = (3.4 \pm 0.3) \times 10^{-5}, \tag{4.2}$$

but we wish to be very conservative to draw secure limits on tensor-scalar gravity. We shall, however, comment below on the effect that a more precise knowledge of the primordial Deuterium abundance, of the type of Eq. (4.2), would have on our results. The minimum value for Lithium 7 is taken from Ref. [14], while the maximum one is the extreme value chosen in Ref. [13]. Finally, we have also computed the BBN yield of Helium 3. We used an extreme range on the (observationally better controlled) sum  $(\text{D} + {}^3\text{He})/\text{H}$ . However, we found that the corresponding limits do not give constraints going beyond those deduced from the BBN yields of Helium 4, Deuterium and Lithium.

### B. Small $\beta$ case (constant speed up factor)

Let us first consider the case where the curvature parameter  $\beta$  of the quadratic coupling function (2.10) is small, say  $\beta \leq 0.2$ . In the limit  $\beta \rightarrow 0$ ,  $\alpha_{\text{quad}}(\varphi) = \beta \varphi \rightarrow 0$ , and the evolution equation (3.22) for  $\varphi$  becomes simply  $\ddot{\varphi} + 3H_* \dot{\varphi} = 0$ . The generic solution  $\varphi$  of this equation tends to an arbitrary constant  $\varphi = C$  as time evolves in the (normal) positive direction. [The other solution is the decreasing mode  $\dot{\varphi}_{\text{dec}} = D/R_*^3$  which is quickly damped away.] It was shown in Ref. [10] that such a behaviour,  $\varphi \simeq \text{constant}$ , is a good approximation to what happens during the  $e^+e^-$  annihilation era *when  $\beta$  is small*. Indeed,

Eqs. (4.20), (4.21) of Ref. [10] show that the *fractional* change of  $\varphi$  across the  $e^+e^-$  threshold is of order  $\Delta_e \varphi/\varphi \sim -k_e \beta \simeq -0.16 \beta$ , where the smallish coefficient  $k_e$  is proportional to the ratio of the number of helicity states of an electron to the total number of relativistic degrees of freedom when  $\tilde{T} > \tilde{m}_e$ . If we limit ourselves to values of  $\beta \leq 0.2$ , the fractional change of  $\varphi$  will be less than 3% and can be neglected. This means that, when  $\beta \leq 0.2$ , the effect of tensor-scalar gravity on BBN is simply obtained by replacing  $\varphi$  by a constant  $\varphi_{\text{in}}$  and  $\chi = \dot{\varphi}$  by 0 in Eqs. (3.8) and (3.11) giving the physical expansion rate. This yields

$$\tilde{H}_{(\text{small } \beta)} = \sqrt{\frac{8\pi G_*}{3} A^2(\varphi_{\text{in}}) \tilde{\rho}}. \quad (4.3)$$

By comparison, the standard value of the expansion rate in general relativity would read

$$\tilde{H}^{\text{standard}} = \sqrt{\frac{8\pi}{3} \tilde{G}_N \tilde{\rho}}, \quad (4.4)$$

where  $\tilde{G}_N$  is the presently observed value of Newton's constant (as measured in Cavendish-type experiments). The value of this observable quantity in tensor-scalar gravity is

$$\tilde{G}_N = \tilde{G}_0 = G_* A^2(\varphi_0) [1 + \alpha_0^2]. \quad (4.5)$$

Therefore, the small- $\beta$  limit of the tensor-scalar expansion rate is obtained from the standard value by the following rescaling of the standard gravitational constant [10]

$$g \equiv \frac{G_* A^2(\varphi_{\text{in}})}{\tilde{G}_0} = \frac{A^2(\varphi_{\text{in}})}{A^2(\varphi_0) [1 + \alpha_0^2]}. \quad (4.6)$$

Equivalently, one could say that the expansion rate (4.3) differs from its standard counterpart by a constant “speed up” factor  $\xi \equiv \tilde{H}/\tilde{H}^{\text{standard}} = \sqrt{g}$ . In our quadratic model (2.10), the natural logarithm of  $g$  reads, in terms of  $\alpha_{\text{in}} = \alpha(\varphi_{\text{in}}) = \beta \varphi_{\text{in}}$ ,

$$\ln g = \frac{1}{\beta} (\alpha_{\text{in}}^2 - \alpha_0^2) - \ln(1 + \alpha_0^2) \simeq \frac{1}{\beta} (\alpha_{\text{in}}^2 - \alpha_0^2) - \alpha_0^2. \quad (4.7)$$

Here, we used the fact that  $\alpha_0^2 \ll 1$ , as known observationally, and also consistently deduced below from BBN data. To express  $\ln g$  in terms of  $\alpha_0$  and  $\beta$  we need to relate  $\alpha_0$  and  $\alpha_{\text{in}}$ . In our present approximation,  $\alpha_{\text{in}} = \beta \varphi_{\text{in}} \simeq \alpha_{\text{out}} = \beta \varphi_{\text{out}}$ , where  $\varphi_{\text{out}}$  is the value of  $\varphi$  at the end of nucleosynthesis. The link between  $\varphi_{\text{out}}$  and the present value  $\varphi_0$  of the scalar field is obtained by integrating Eq. (3.22) (with initial conditions  $\varphi = \varphi_{\text{out}}$ ,  $\dot{\varphi} = 0$ ) from the end of nucleosynthesis up till the present time. The evolution of  $\varphi$  during this time span comes from its coupling to the total matter (baryons plus cold dark matter). The corresponding scalar source  $\sigma_{*m} = \rho_{*m} - 3p_{*m} \simeq \rho_{*m}$  has a small effect on the evolution of  $\varphi$  during the radiation era but becomes very important during the subsequent matter-dominated era. It was very generally shown in Ref. [10] that the  $t_*$ -time evolution equation (3.12) for  $\varphi$  (which must *a priori* be solved together with the evolution equation for the scale factor  $R_*$ ) can be conveniently rewritten as a decoupled equation for the evolution of  $\varphi$  with respect to the parameter

$$p = \int H_* dt_* = \ln R_* + \text{cst} , \quad (4.8)$$

which measures the number of  $e$ -folds in the Einstein frame. The latter  $p$ -time equation was approximately solved in Ref. [10] for the present case of the transition between the radiation era and the matter era. For simplicity, and because it is the theoretically most plausible value, we assume here and below that the spatial curvature  $k = 0$ . [ The effect of nonzero curvature has been investigated in Ref. [10].] The result for small  $\beta$  reads

$$\frac{\varphi_0}{\varphi_{\text{out}}} = \frac{\alpha_0}{\alpha_{\text{out}}} \simeq \frac{1+r}{2r} \exp \left[ -\frac{3}{4} (1-r) p_0 \right] \simeq e^{-\beta p_0} . \quad (4.9)$$

Here,  $r \equiv \sqrt{1 - 8\beta/3} = 1 - 4\beta/3 + \mathcal{O}(\beta^2)$ , and

$$p_0 \equiv \ln(R_{*0}/R_*^{\text{equivalence}}) , \quad (4.10)$$

denotes the number of Einstein-frame  $e$ -folds separating the present moment from the time of equivalence between matter and radiation:  $1 = (\rho_{*m}/\rho_{*\text{rad}})^{\text{equivalence}} = (\tilde{\rho}_m/\tilde{\rho}_{\text{rad}})^{\text{equivalence}}$ . The corresponding *physical* redshift is

$$\tilde{Z}_0 = \frac{\tilde{R}_0}{\tilde{R}^{\text{equivalence}}} = \frac{\tilde{\rho}_m^0}{\tilde{\rho}_{\text{rad}}^0} = 2.404 \times 10^4 \Omega_m h^2 . \quad (4.11)$$

Here,  $\Omega_m \equiv \tilde{\rho}_m^0/\tilde{\rho}_c^0$  is the present ratio of the total matter density to the (physical-units) ‘‘closure density’’  $\tilde{\rho}_c^0 = 3\tilde{H}_0^2/(8\pi\tilde{G}_0)$  and  $h \equiv \tilde{H}_0/(100 \text{ kms}^{-1} \text{ Mpc}^{-1})$  is the reduced Hubble parameter. Note that the product

$$\Omega_m h^2 = \frac{\tilde{\rho}_m^0}{1.879 \times 10^{-29} \text{ g cm}^{-3}} , \quad (4.12)$$

is independent from the value of  $\tilde{H}_0$  and depends only on the actual value of the total matter density. Finally, using the link (3.6b) between  $\tilde{R}$  and  $R_*$ , the number of Einstein-frame  $e$ -folds (4.10) reads [10]

$$p_0 = \ln \tilde{Z}_0 + a(\varphi_{\text{out}}) - a(\varphi_0) , \quad (4.13)$$

which gives numerically

$$\begin{aligned} p_0 &= 10.09 + \ln(\Omega_m h^2) + a(\varphi_{\text{out}}) - a(\varphi_0) \\ &= 8.19 + \ln(\Omega_m h^2/0.15) + a(\varphi_{\text{out}}) - a(\varphi_0) . \end{aligned} \quad (4.14)$$

Here, we introduced as fiducial value for the matter density the value  $(\Omega_m h^2)^{\text{fiducial}} = 0.15$  which corresponds roughly to the currently favoured values  $\Omega_m \sim 0.3$ ,  $h \simeq 0.7$  (it could also correspond to  $\Omega_m \simeq 1$ ,  $h \simeq 0.4$ ).

Using the link (4.9) we can express  $\alpha_{\text{in}}$ , in Eq. (4.7), in terms of  $\alpha_0$ :  $\alpha_{\text{in}} \simeq \alpha_{\text{out}} \simeq e^{+\beta p_0} \alpha_0$ . This gives

$$\ln g \simeq \frac{\alpha_0^2}{\beta} [e^{2\beta p_0} - 1 - \beta] . \quad (4.15)$$

Note that, though we are considering here smallish values of  $\beta \sim 0.1$ , we are not entitled to expanding the exponential in Eq. (4.15). Indeed, we see from Eq. (4.14) that  $2p_0 \sim 16$  is rather large. When  $\beta$  is very small (with  $2p_0\beta \ll 1$ ), the expansion of the R.H.S. of Eq. (4.15) gives a finite limit

$$(\ln g)_{\beta \rightarrow 0} = (2p_0 - 1) \alpha_0^2. \quad (4.16)$$

It is easily checked that the R.H.S. of Eq. (4.15) is positive (because  $p_0 > 1/2$ ). Therefore, we conclude that, in the limit of small  $\beta$ , tensor-scalar gravity leads to speeding up the expansion rate:  $\xi = \sqrt{g} > 1$ . It is, however, interesting to leave first unrestricted the sign of  $\ln g$  and to study the effect on BBN of replacing  $\tilde{G}_N \rightarrow g \tilde{G}_N$  for both signs of  $\ln g$ . We have run BBN codes with varying values of  $g$  and  $\eta = \tilde{n}_b/\tilde{n}_\gamma$ , and computed the resulting abundances of light elements, comparing them to the extreme observational ranges given in Eqs. (4.1). The results of this comparison are given in Fig. 1 which represents the allowed regions in the  $(\eta, g)$  plane. The total phenomenologically allowed range for  $g$  would be  $g_{\min} < g < g_{\max}$  with

$$g_{\min} \simeq 0.64, \quad g_{\max} \simeq 1.27. \quad (4.17)$$

In our case  $g$  is restricted to be larger than one and we have the firm constraint  $1 \leq g < g_{\max}$ . Note that the maximum allowed value of  $g$  is constrained by the upper bound on the deuterium, combined with the upper bound on Helium 4. To illustrate the effect of choosing a much smaller range for deuterium, we have also plotted on Fig. 1 (in dashed lines) the limits on  $g$  obtained by using as confidence interval the  $(1\sigma)$  one suggested by the recent results of Tytler and collaborators [31], Eq. (4.2). This would give the stronger constraint  $g_{\max} \simeq 1.1$ .

Note also that the shapes of the curves bounding the maximally allowed region are such that, when  $g$  is only allowed to vary above one, the corresponding allowed interval for the values of the baryon to photon ratio  $\eta_{10} \equiv 10^{10} \times \eta$  does not change significantly: roughly  $1.5 < \eta_{10} < 8.5$ . Therefore, when  $\beta < 0.2$ , the addition of a scalar component to gravity does not change the upper bound on  $\Omega_b h^2$  deduced from BBN. The case  $\beta > 0.2$  will be considered below.

Let us now turn to the constraints on the parameters  $\alpha_0$  and  $\beta$  of tensor-scalar gravity following from BBN. Using the result (4.15), the constraint  $1 \leq g < g_{\max}$  translates in the following bound on  $\alpha_0^2$

$$\alpha_0^2 < \frac{\beta}{e^{2\beta p_0} - 1 - \beta} \ln g_{\max}. \quad (4.18)$$

In particular, the limit (4.16) when  $\beta \ll 1/(2p_0)$  yields

$$(\alpha_0^2)_{\beta \rightarrow 0} < \frac{1}{2p_0 - 1} \ln g_{\max}, \quad (4.19)$$

which is numerically of order  $(\alpha_0^2)_{\beta \rightarrow 0} \lesssim 0.015$ . Note that, given a value of  $\Omega_m h^2$ , the precise value of  $p_0$  defined by Eq. (4.14) must be obtained by iteration because the small (but non negligible) additional term

$$a(\varphi_{\text{out}}) - a(\varphi_0) = \frac{\alpha_{\text{out}}^2 - \alpha_0^2}{2\beta} = \frac{e^{2\beta p_0} - 1}{2\beta} \alpha_0^2, \quad (4.20)$$

depends both on  $\alpha_0$  and on  $p_0$ . However, in our present approximation of small  $\beta$ , we can replace (4.18) in (4.20) to get

$$(a_{\text{out}} - a_0)_{\text{small } \beta}^{\text{maximum}} = \frac{e^{2\beta p_0} - 1}{2(e^{2\beta p_0} - 1 - \beta)} \ln g_{\text{max}} \simeq \frac{1}{2} \ln g_{\text{max}}. \quad (4.21)$$

We then deduce from this result that the value of  $p_0$  which can be used for estimating the maximum BBN-allowed  $\alpha_0^2$  is

$$\begin{aligned} (p_0)_{\text{small } \beta} &\simeq 8.19 + \ln(\Omega_m h^2/0.15) + \frac{1}{2} \ln g_{\text{max}} \\ &\simeq 8.31 + \ln(\Omega_m h^2/0.15). \end{aligned} \quad (4.22)$$

### C. $\beta > 0.2$ case

Let us now consider the complementary case where  $\beta > 0.2$ . In this case, the total attraction due to the matter era is quite large. Indeed, the ratio  $\alpha_0^2/\alpha_{\text{out}}^2$  decreases fast with  $\beta$ , and even for  $\beta = 0.2$ , one finds from Eq. (4.9)  $\alpha_0^2/\alpha_{\text{out}}^2 \simeq e^{-2\beta p_0} \sim 0.04$ , where we used  $p_0 \sim 8$ . Therefore, when  $\beta \geq 0.2$  we can, as was mentioned in Section 3, neglect the difference between  $G_*$  and  $\tilde{G}_0 = G_* A^2(\varphi_0)[1 + \alpha_0^2]$ . This allows one to run (in the forward time direction) the tensor-scalar-modified BBN code described in Section 3, with the numerical value  $G_* \simeq 6.672 \times 10^{-8} \text{ cm}^3 \text{ g}^{-1} \text{ s}^{-2}$ . Let us recall that the input parameters which must be chosen in each run are:  $\beta$ , the baryon-to-photon ratio  $\eta_{10} = 10^{10} \times \eta$ , and the value  $\varphi_{\text{in}}$  of the scalar field before freeze-out and  $e^+e^-$  annihilation. Instead of working with  $\varphi_{\text{in}}$ , it is physically more appropriate to work with the corresponding value of the (logarithmic) coupling function  $a_{\text{in}} \equiv a(\varphi_{\text{in}}) = \frac{1}{2} \beta \varphi_{\text{in}}^2$ . For each value of the triplet  $(\beta, \eta, a_{\text{in}})$ , the code then computes the abundances of light elements produced by the BBN, and the value  $\varphi_{\text{out}}$  of the scalar field after the end of nucleosynthesis (together with the corresponding  $a_{\text{out}} = a(\varphi_{\text{out}})$  and  $\alpha_{\text{out}} = \alpha(\varphi_{\text{out}})$ ). Let us recall that for temperatures well above and well below the electron-annihilation threshold  $\tilde{T} \sim \tilde{m}_e$ , the source term  $\tilde{\sigma}_e$  on the R.H.S. of the evolution equation (3.13b) for  $\varphi$  becomes negligible, while the friction term remains, so that  $\varphi$  stops evolving. [This approximation is correct as long as  $\tilde{T} \ll \tilde{m}_\mu$  and  $\tilde{T} \gg \tilde{T}_{\text{equivalence}}$ .] On the other hand, when  $\tilde{T}$  is between  $5\tilde{m}_e \sim 2.5 \text{ MeV}$  and  $0.2\tilde{m}_e \sim 0.1 \text{ MeV}$ , which is a crucial period during which weak interactions freeze (the  $(n/p)$  ratio freezes out around  $\tilde{T} \sim 0.8 \text{ MeV}$ ), and nuclear reactions start to build up light elements, the source term  $\tilde{\sigma}_e$  is numerically important and causes  $\varphi$  to oscillate around  $\varphi = 0$ . As discussed in detail in Ref. [11] these oscillations are very vigorous when  $\beta \gg 1$ . Therefore, we have a physically non trivial situation where the physical cosmological expansion rate  $\tilde{H}$  (given in terms of  $\varphi$  by Eqs. (3.8) and (3.11)) varies in a complicated manner precisely during the crucial stages of BBN. This situation cannot be analytically approximated, and must be tackled numerically. We can visualize the results of our numerical simulations by representing, for

each value of  $\beta$ , the contour levels of the light element abundances in the  $(\eta, a_{\text{in}})$  plane. The topology of these contour levels depend on how large  $\beta$  is.

When  $\beta \lesssim 16$ , the contour levels look like continuously deformed versions of the small- $\beta$  case, i.e. the case of a constant speed up factor  $\xi = \sqrt{g}$  shown above in Fig. 1. For instance, the case  $\beta = 10$  is shown in Fig. 2 and should be compared with the part of Fig. 1 above the  $g = 1$  line. Therefore, when  $\beta \lesssim 16$  the upper bound on the value of  $a_{\text{in}}$  is given, as in the small- $\beta$  case, by the upper left corner of the “triangle” defined by the  $(\text{D}/\text{H})_{\text{max}}$  and the  $\text{He}_{\text{max}}$  lines. We have checked that there is approximate continuity between the small- $\beta$  case and the  $\beta > 0.2$  case: Indeed, by running a BBN code for  $\beta = 0.2$  we find a maximum allowed value  $a_{\text{in}}^{\text{max}} = 0.125$  (together with a corresponding  $a_{\text{out}}^{\text{max}} \simeq 0.109$ ) which approximately agrees with  $\frac{1}{2} \ln g_{\text{max}} \simeq 0.12$ , for the  $g_{\text{max}} \simeq 1.27$  obtained above in the small- $\beta$  approximation. [Here, we used Eq. (4.7), in which we neglected the fractionally small  $\alpha_0^2$  terms.] As in the small- $\beta$  case, we find that the shapes of the curves bounding the allowed region are such that the corresponding allowed interval for  $\eta_{10}$  does not change significantly.

When  $\beta \gtrsim 16$ , the “triangle” of Fig. 2 disappears because many of the contour lines tend to straighten out and become parallel. This situation is illustrated in Fig. 3 for  $\beta = 40$ . This case illustrates two interesting phenomena. First, though the shapes of the contours have changed a lot, they are still such that the allowed interval for  $\eta_{10}$  does not change significantly: roughly,  $1.5 < \eta_{10} < 8.5$ . Second, Fig. 3 shows that the initial value  $a_{\text{in}}$ , i.e. the initial speed-up factor  $\xi_{\text{in}} = A_{\text{in}}/(A_0\sqrt{1 + \alpha_0^2}) \simeq A_{\text{in}} = \exp(a_{\text{in}})$  can be extremely large (for instance, the largest value  $a_{\text{in}} \simeq 5$  of Fig. 3 corresponds to  $\xi_{\text{in}} \simeq 150$ , and much larger values are possible) and still lead to compatibility with the observed abundances of light elements. This result contradicts the usual expectation that the BBN data are tight enough to constrain to a small level any deviation from standard gravity around the epoch of BBN. Here, we have an example where, just before the BBN starts, the tensor-scalar-predicted expansion rate is several orders of magnitude larger than the Einstein-predicted one, and where the BBN test is still passed. This paradoxical result raises two questions: (i) How can an abnormally large expansion rate, around the (nominal) time of freeze-out of the neutron to proton ratio, lead to quasi-normal light element abundances?; and, (ii) Does this imply that, when  $\beta \gtrsim 16$ , the present value of  $\alpha_0^2$  (which measures the deviation between general relativity and tensor-scalar gravity) can be large?

To answer the first question, we plot in Fig. 4 the coupling function  $a(\varphi)$ , which is essentially the logarithm of the speed-up factor, as a function of the inverse (physical) temperature  $1/\tilde{T}$  (we use as input values  $\beta = 40$ , and  $a_{\text{in}} = 2$ ). We plot on the same Figure the evolution with temperature of: the actual neutron to proton ratio in tensor-scalar theory (solid line), the  $(n/p)$  ratio in the standard general relativistic case (dashed line), and the instantaneous equilibrium value for this ratio:  $(n/p)_{\text{eq}} = \exp(-Q/\tilde{T})$ , where  $Q \equiv \tilde{m}_n - \tilde{m}_p \simeq 1.293$  MeV (dotted line). If we define (as is often done) a nominal freeze-out temperature as the temperature  $\tilde{T}_*$  where the actual  $(n/p)$  ratio starts to deviate significantly from  $(n/p)_{\text{eq}}$  (a sign that weak interactions become slow compared to the expansion rate), we see that the value of  $\tilde{T}_*$  in tensor-scalar gravity is larger than in general relativity, as expected from the fact that the expansion rate is much larger ( $a(\varphi)$  being initially frozen at  $a \simeq a_{\text{in}} = 2$ ). If that were all, this would lead to a significantly larger value for the  $(n/p)$  ratio. However, Fig. 4 illustrates two physical phenomena that modify this naive conclusion.



First, around  $\tilde{T} \sim 0.8$  MeV, the source term  $\tilde{\sigma}_e$  starts to have a strong effect on  $a(\varphi)$ : it makes  $a(\varphi)$  drop precipitously toward zero, where it bounces twice to end up being frozen (when  $\tilde{T} \lesssim 1/20$  MeV) at a very small limiting value  $a_{\text{out}} \simeq 0.016$ . The second important phenomenon illustrated by Fig. 4 is the fact that the freeze-out phenomenon is not something which takes place at a precise moment in time, but is an integrated phenomenon. It is clear from the Figure that the approximate plateau reached by  $(n/p)$  (before it drops around 1/15 MeV when nuclear reactions start) is due to the integrated effect of an evolution which takes place before, during and after the precipitous fall of  $a(\varphi)$  toward small values. It is therefore impossible to estimate analytically the final “plateau” value of  $(n/p)$  from the sole knowledge of the nominal freeze-out temperature. In particular, we see that  $(n/p)$  is initially larger than the standard GR value, but ends up, in this example, being somewhat smaller. This Figure illustrates the necessity of resorting to a full numerical BBN code.

Let us now address the second question: What does an initially large value of  $a_{\text{in}} = a(\varphi_{\text{in}})$  imply for the present value of  $\alpha_0^2$ ? Can  $\alpha_0^2$  be large? The answer is no, for the following reason: when  $\beta$  is large, the source  $\tilde{\sigma}_e$ , active around  $\tilde{T} \sim \tilde{m}_e$ , is very efficient in attracting  $\varphi$  toward zero (through a damped-oscillatory evolution). Moreover this attraction effect is amplified by nonlinearities so that, for a fixed  $\beta$ , the post-BBN value  $a_{\text{out}} = a(\varphi_{\text{out}})$  does not increase monotonically with  $a_{\text{in}} = a(\varphi_{\text{in}})$ , but rather decreases for large  $a_{\text{in}}$  values after having reached a maximum when  $a_{\text{in}} \sim 1$ . This behaviour is illustrated in Fig. 5. We see from this Figure that, in the plane of Fig. 3,  $a_{\text{out}}$  (considered as a function of  $a_{\text{in}}$ ) reaches the maximum value  $a_{\text{out}}^{\text{max}} \simeq 0.028$  when  $a_{\text{in}} \simeq 0.7$ .

For some particular values of  $\beta$  (near 23, 59, ...) the curve giving  $a_{\text{out}}$  versus  $a_{\text{in}}$  develops a second maximum which becomes higher than the first (like in a first-order phase transition). This is illustrated in Fig. 6 which shows the evolution of the curves between  $\beta = 22, 23$  and 24, and between  $\beta = 58, 59$  and 60. In both cases, the formerly unique maximum located near the origin gets superseded, roughly when its location along the  $a_{\text{in}}$  axis decreases down to  $\sim 0.2$ , by a secondary maximum (which develops abruptly for  $\beta \gtrsim 21$ , or  $\beta \gtrsim 56$ ) located around  $a_{\text{in}} \sim 1.7$ . As  $\beta$  further increases, the first maximum gets very small and disappears, while the position, along the  $a_{\text{in}}$  axis, of the second maximum continuously slides toward the left (so that the “first maximum” in the bottom panel of Fig. 5 is the evolved form of the second maximum in the top panel).

In all cases, the maximum possible value of  $a_{\text{out}}$ , or better of the difference  $a_{\text{out}} - a_0$  (which matters most when  $\beta$  is small), i.e. the maximum deviation from general relativity *after* the end of nucleosynthesis, compatible with BBN data, is quite small. This is shown in Fig. 7 which plots the maximum allowed  $a_{\text{out}} - a_0$  in function of  $\beta$ . When  $\beta > 0.2$ , the maximum value of  $a_{\text{out}} - a_0 \simeq a_{\text{out}}$  is obtained from the results of the present sub-section, while for  $\beta < 0.2$ ,  $a_{\text{out}} - a_0$  is obtained from the small- $\beta$  result, Eq. (4.21).

## V. BBN LIMITS ON THE PRESENT DEVIATIONS FROM EINSTEIN'S THEORY

In the previous Section, we have shown what limit BBN data put on  $a_{\text{out}} = a(\varphi_{\text{out}})$  as a function of  $\beta$ . It remains to translate this limit on the value of  $\varphi$  at the end of nucleosynthesis into a limit on the present scalar-coupling parameter  $\alpha_0 = \alpha(\varphi_0)$ . To do this we need to

integrate the  $\varphi$ -evolution through the transition between the radiation era and the matter era, up till now. As we said above,  $\varphi$  satisfies a decoupled equation in terms of the parameter  $p$  of Eq. (4.8) [10]. In the present case of the transition between the radiation era and the matter era, it was further shown in Ref. [11] that the latter  $p$ -time decoupled evolution equation can be approximately rewritten as the following hypergeometric equation

$$x(x+1)\partial_x^2\varphi + \left(\frac{5}{2}x+2\right)\partial_x\varphi + \frac{3}{2}\beta\varphi = 0. \quad (5.1)$$

Here  $x \equiv e^p \equiv R_*(t_*)/R_*^{\text{equivalence}}$  denotes the (Einstein frame) redshift separating the current time  $t_*$  from the time of equivalence (when  $\rho_{*m}(t_*^{\text{equivalence}}) = \rho_{*\text{radiation}}(t_*^{\text{equivalence}})$ ). The initial conditions for  $\varphi$ , deep into the radiation era (i.e. for  $x \rightarrow 0$ ), mentioned in Section IVB above, select uniquely the solution  $\varphi(x) = \varphi_{\text{out}} F[a, b, c; -x]$ . Here,  $F[a, b, c; z]$  denotes the usual (Gauss) hypergeometric series. The values of the parameters are

$$a = \frac{3}{4} - i\omega, \quad b = \frac{3}{4} + i\omega, \quad c = 2; \quad \omega \equiv \sqrt{\frac{3}{2}\left(\beta - \frac{3}{8}\right)}. \quad (5.2)$$

Finally the ratio between the present value of  $\varphi$  and its value at the end of nucleosynthesis,

$$\frac{\varphi_0}{\varphi_{\text{out}}} = \frac{\alpha_0}{\alpha_{\text{out}}} \equiv F_m(\beta, Z_{*0}) \quad (5.3)$$

is given by

$$F_m = F[a, b, c; -Z_{*0}] \simeq \frac{\sqrt{2}}{\sqrt{\pi}} 2^{2i\omega} \frac{\Gamma(2i\omega)}{\Gamma\left(2i\omega + \frac{3}{2}\right)} e^{-\frac{3}{4}p_0} e^{i\omega p_0} + (i\omega \leftrightarrow -i\omega). \quad (5.4)$$

In the last form (made of two terms obtained by changing the sign of  $\omega$ ) we have used the asymptotic behaviour, for large argument, of the hypergeometric function. Here,  $Z_{*0} \equiv e^{p_0}$  denotes the Einstein-frame redshift separating the present moment from equivalence. Its natural logarithm  $p_0 = \ln Z_{*0}$  is given by Eq. (4.14). The result (5.4) is valid both when  $\beta < 3/8$  (in which case  $\omega$  is pure imaginary, with  $i\omega = \sqrt{\frac{3}{2}\left(\frac{3}{8} - \beta\right)}$ ) and when  $\beta > 3/8$  ( $\omega$  real). It is easily checked that when  $\beta$  is small the result (5.4) agrees with the more approximate Eq. (4.9). Using Eq. (5.3) we can compute  $\alpha_0^2$  in terms of  $a_{\text{out}} = \frac{1}{2}\beta\varphi_{\text{out}}^2 = \alpha_{\text{out}}^2/(2\beta)$

$$\alpha_0^2 = F_m^2(\beta, Z_{*0}) \alpha_{\text{out}}^2 = 2\beta F_m^2(\beta, Z_{*0}) a_{\text{out}}. \quad (5.5)$$

Using Eq. (5.5) we can, for a given value of  $Z_{*0}$ , translate the BBN limit of Fig. 7 on  $a_{\text{out}} - a_0$  into a limit on the present scalar-coupling parameter  $\alpha_0^2$ . As before, when  $\beta > 0.2$ ,  $a_{\text{out}} - a_0 \simeq a_{\text{out}}$  and the limit on  $\alpha_0^2$  is obtained from Eq. (5.5), while, when  $\beta < 0.2$ , one uses the small- $\beta$  limit, Eq. (4.18). This limit is represented in Fig. 8 (solid line) for our fiducial value  $\Omega_m h^2 = 0.15$ , in Eq. (4.14). The corresponding limit on the product  $\beta\alpha_0^2$  is represented in Fig. 9. We recall from Eqs. (2.9) that the quantities represented in Figs. 8 and 9 are directly related to the parameters measuring post-Newtonian deviations from general relativity. As  $\alpha_0^2 \ll 1$ , we have  $\bar{\gamma} \equiv \gamma_{\text{Edd}} - 1 \simeq -2\alpha_0^2$ , and  $\bar{\beta} \equiv \beta_{\text{Edd}} - 1 \simeq \frac{1}{2}\beta\alpha_0^2$ .

For comparison let us recall the current direct experimental limits on  $\alpha_0^2$  and  $\beta \alpha_0^2$ . The measurement of the Shapiro time delay by the Viking mission [32], as well as some VLBI measurements [33], yield the  $1\sigma$  bound  $|\bar{\gamma}| < 2 \times 10^{-3}$  which translates into  $\alpha_0^2 < 10^{-3}$ . A more stringent limit follows from the Lunar Laser Ranging experiment [34] which yields the  $1\sigma$  bound  $-1.7 \times 10^{-3} < 4\bar{\beta} - \bar{\gamma} < 3 \times 10^{-4}$ . This translates into

$$-8.5 \times 10^{-4} < (1 + \beta_0) \alpha_0^2 < 1.5 \times 10^{-4} (1\sigma). \quad (5.6)$$

In the framework of the present paper, the parameter  $\beta_0 = \beta$  is restricted to be positive. Therefore, the most stringent limit is the right inequality in Eq. (5.6), i.e.

$$\alpha_0^2 < \frac{1.5 \times 10^{-4}}{\beta + 1}, \quad \beta \alpha_0^2 < \frac{\beta}{\beta + 1} 1.5 \times 10^{-4}. \quad (5.7)$$

[Strong-field tests put also limits on  $\alpha_0^2$  but they are slightly less stringent than the above when  $\beta$  is positive [9].] We have indicated on Figs. 8 and 9 the empirical bounds (5.7) in dashed lines.

Figs. 8 and 9 show that BBN data put, as soon as  $\beta > 0.3$ , more stringent limits on the possible post-Newtonian deviations from general relativity than present experimental data. For our fiducial matter density  $\Omega_m h^2 = 0.15$  the level of deviation compatible with BBN data is (for  $\beta \gtrsim 0.5$ ) constrained to the level  $\beta \alpha_0^2 \lesssim 10^{-6.5}$ . As discussed in Ref. [10] the attraction factor  $F_m^2(\beta, Z_{*0})$  in Eq. (5.5) scales (for  $\beta > 3/8$ ) like  $(\Omega_m h^2)^{-3/2}$ . Note that the corresponding deviation level  $\alpha_0^2 \lesssim 10^{-6.5} \beta^{-1} (\Omega_m h^2 / 0.15)^{-3/2}$  gets significantly smaller if  $\Omega_m h^2$  turns out to be of order one. Note finally that the attraction factor  $F_m$  is dominated by the evolution during the matter-dominated era and is only negligibly modified (in view of our other approximations) if one takes into account the fact that our recent cosmological evolution may have been curvature-dominated [10] or  $\Lambda$ -dominated.

## VI. CONCLUSIONS

The most natural, and best motivated, alternatives to general relativity are the tensor-scalar theories of gravitation. We have considered the class of tensor-scalar theories which are dynamically attracted, during their cosmological evolution, toward general relativity. The paradigmatic example of this class is defined by the quadratic coupling function  $a(\varphi) = \frac{1}{2} \beta \varphi^2$  with positive  $\beta$ . We studied Big Bang Nucleosynthesis in this quadratic model as a function of  $\beta$ , of the initial value  $\varphi_{\text{in}}$  (at temperatures  $\sim 10$  MeV) of the scalar field, and of the baryon-to-photon ratio  $\eta$ . [We assume three light neutrinos throughout this work.] We imposed that the theoretically predicted BBN yields of light elements (Deuterium, Helium 4 and Lithium 7) be compatible with some conservative ranges for the corresponding observed primordial abundances, Eqs. (4.1).

Our first conclusion is that the BBN-inferred upper bound on the cosmological baryon density  $\Omega_b h^2 = 3.66 \times 10^7 (\tilde{T}_0 / 2.726 \text{ K})^3 \eta$  is quite robust under the addition of a scalar component to gravity. The standard bounds on  $\eta_{10} \equiv 10^{10} \eta$ , namely  $1.5 < \eta_{10} < 8.5$ , corresponding to  $0.0055 < \Omega_b h^2 < 0.031$ , are insignificantly modified even when considering large initial values of the scalar field, corresponding to an initial cosmological expansion

rate much larger than its standard general relativistic value. This is strikingly illustrated in Fig. 3.

Our second conclusion is that, even in the cases where, before BBN, tensor-scalar gravity is very different from Einstein’s gravity, the presently observable deviations from general relativity are constrained by BBN to be quite small. The BBN-limits on the two independent weak-field “post-Einstein” parameters  $\alpha_0^2$  and  $\beta \alpha_0^2$  (linked to the usual post-Newtonian parameters through  $\gamma_{\text{Edd}} - 1 \simeq -2\alpha_0^2$ ,  $\beta_{\text{Edd}} - 1 \simeq \frac{1}{2}\beta \alpha_0^2$ ) are exhibited in Fig. 8 and Fig. 9, in the fiducial case where the total matter density is  $\Omega_m h^2 = 0.15$ . The BBN-limits in Fig. 8 and 9 scale (for  $\beta > 3/8$ ) like  $(\Omega_m h^2/0.15)^{-3/2}$ . The dashed lines in Figs. 1, 2 and 3 show also that if, in the future, one gets more stringent bounds on the Deuterium primordial abundance this will tighten the BBN-limits on  $\alpha_0^2$  for  $\beta \lesssim 16$ , without affecting them for  $\beta \gtrsim 16$ . As soon as  $\beta \gtrsim 0.3$  the BBN-limits we obtain on possible deviations from Einstein’s theory are much stronger than the present observational limits from solar-system or binary-pulsar gravitational experiments. They provide motivations for experiments which push beyond the present empirical bounds on the basic scalar coupling parameter  $\alpha_0^2$ .

### ACKNOWLEDGMENTS

We thank Rocky Kolb for kindly providing us with a copy of the Wagoner-Kawano BBN code, Yvon Biraud for helpful advice on several numerical issues, and Bob Wagoner for useful comments.

## REFERENCES

- [1] T. Kaluza, Sitzungsber. der K. Preuss. Akad. der Wiss. zu Berlin, p. 966 (1921).
- [2] P. Jordan, Nature **164**, 637 (1949); *Schwerkraft und Weltall* (Vieweg, Braunschweig, 1955); Z. Phys. **157**, 112 (1959).
- [3] M. Fierz, Helv. Phys. Acta **29**, 128 (1956).
- [4] C. Brans and R.H. Dicke, Phys. Rev. **124**, 925 (1961).
- [5] K. Nordtvedt, Astrophys. J. **161**, 1059 (1970).
- [6] R.V. Wagoner, Phys. Rev. D **1**, 3209 (1970).
- [7] T. Damour and G. Esposito-Farèse, Class. Quantum Grav. **9**, 2093 (1992).
- [8] M.B. Green, J.H. Schwarz and E. Witten, *Superstring Theory* (Cambridge University Press, Cambridge, 1987).
- [9] T. Damour and G. Esposito-Farèse, Phys. Rev. D **54**, 1474 (1996); and gr-qc/9803031 (to appear in Phys. Rev. D).
- [10] T. Damour and K. Nordtvedt, Phys. Rev. Lett. **70**, 2217 (1993); and Phys. Rev. D **48**, 3436 (1993).
- [11] T. Damour and A.M. Polyakov, Nucl. Phys. B **423**, 532 (1994); Gen. Rel. Grav. **26**, 1171 (1994).
- [12] V.F. Shvartsman, JETP Lett. **9**, 184 (1969).
- [13] H. Reeves, Rev. Mod. Phys. **66**, 193 (1994).
- [14] C.J. Copi, D.N. Schramm and M.S. Turner, Science **267**, 192 (1995).
- [15] L. M. Krauss and P. J. Kernan, Phys. Lett. **B347**, 347 (1995).
- [16] T. Rothman and R. Matzner, Astrophys. J. **257**, 450 (1982).
- [17] T. Damour and C. Gundlach, Phys. Rev. D **43**, 3873 (1991).
- [18] J.A. Casas, J. Garcia-Bellido and M. Quiros, Mod. Phys. Lett. A **7**, 447 (1992).
- [19] G. Steigman, Nature (London) **261**, 479 (1976).
- [20] J.D. Barrow, Mon. Not. R. Astron. Soc. **184**, 677 (1978).
- [21] J. Yang, D.N. Schramm, G. Steigman and R.T. Rood, Astrophys. J. **227**, 697 (1979).
- [22] F.S. Accetta, L.M. Krauss and P. Romanelli, Phys. Lett. B **248**, 146 (1990).
- [23] D.I. Santiago, D. Kalligas and R.V. Wagoner, Phys. Rev. D **56**, 7627 (1997).
- [24] A. Serna and J.M. Alimi, Phys. Rev. D **53**, 3087 (1996).
- [25] T. Damour and G. Esposito-Farèse, Phys. Rev. D **53**, 5541 (1996).
- [26] T. Damour and G. Esposito-Farèse, Phys. Rev. Lett. **70**, 2220 (1993).
- [27] L. Kawano, 1992, Fermilab preprint FERMILAB-PUB-92/04-A, Kellogg Radiation Lab preprint OAP-714, unpublished.
- [28] R.V. Wagoner, Astrophys. J. **179**, 343 (1973).
- [29] D. Sasselov and D. Goldwirth, Astrophys. J. **444**, L5 (1995).
- [30] M. Rugers and C.J. Hogan, Astrophys. J. **459**, L1 (1996).
- [31] S. Burles and D. Tytler, astro-ph/9803071.
- [32] R.D. Reasenberg et al., Astrophys. J. **234**, L219 (1979).
- [33] D.S. Robertson et al., Nature (London) **349**, 768 (1991); D.E. Lebach et al., Phys. Rev. Lett. **75**, 1439 (1995).
- [34] J.G. Williams, X.X. Newhall and J.O. Dickey, Phys. Rev. D **53**, 6730 (1996).

FIGURES

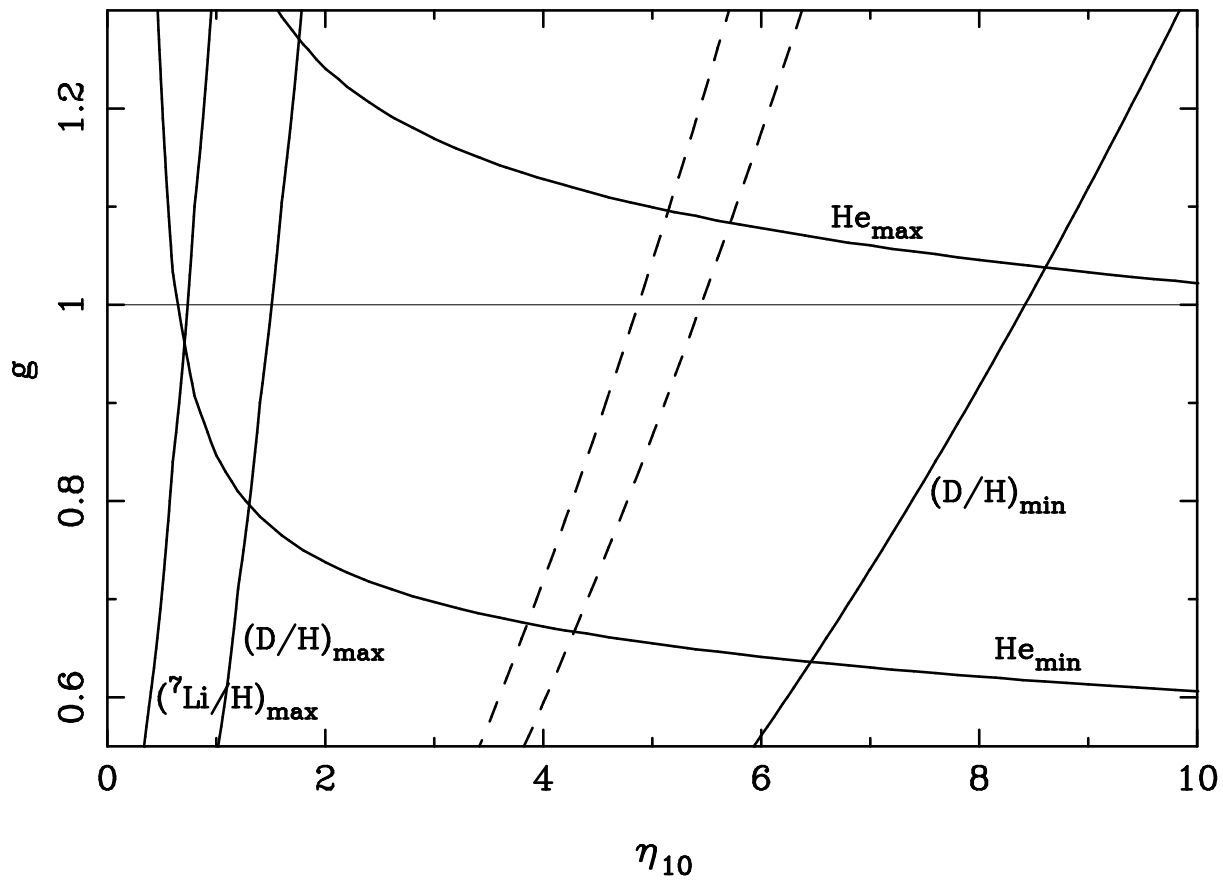


FIG. 1. Level contours of BBN yields as functions of the baryon-to-photon ratio  $\eta_{10} = 10^{10} \eta = 10^{10} \tilde{n}_b / \tilde{n}_\gamma$  and of a (squared) speed-up factor  $g = \xi^2 = \tilde{G}^{\text{effective}} / \tilde{G}_{\text{Newton}}$ . The solid lines correspond to the conservative observational bounds of Eqs. (4.1). The allowed region is the inside of the curved parallelogram defined by the He and D/H lines. The dashed lines, given for illustration, correspond to the Deuterium  $1\sigma$  range of Eq. (4.2).

$$\beta = 10.$$

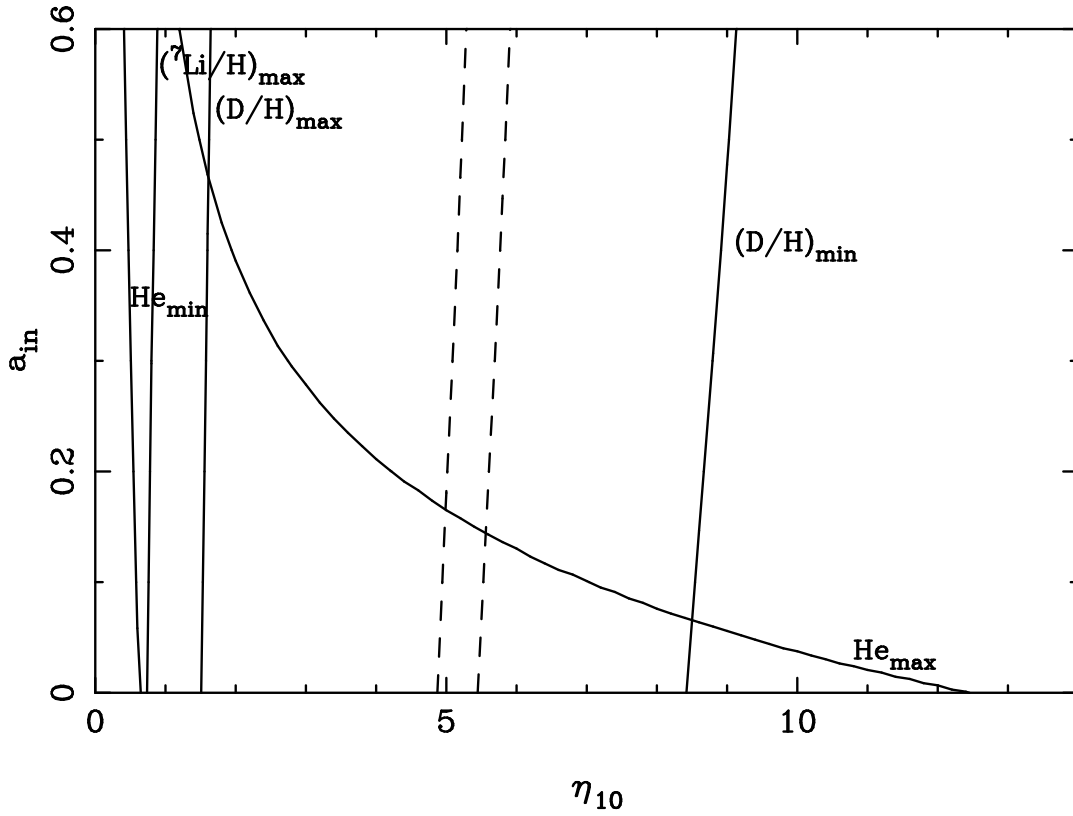


FIG. 2. Level contours of BBN yields when  $\beta = 10$  as functions of the baryon-to-photon ratio  $\eta_{10}$  and of the initial value of the scalar coupling function  $a_{\text{in}} = a(\varphi_{\text{in}})$ . The lines are defined as in Fig. 1. The allowed region for the conservative bounds is the truncated quasi-triangle defined by  $\text{He}_{\text{max}}$ ,  $(\text{D}/\text{H})_{\text{max}}$ ,  $(\text{D}/\text{H})_{\text{min}}$  and the horizontal axis.

$$\beta = 40.$$

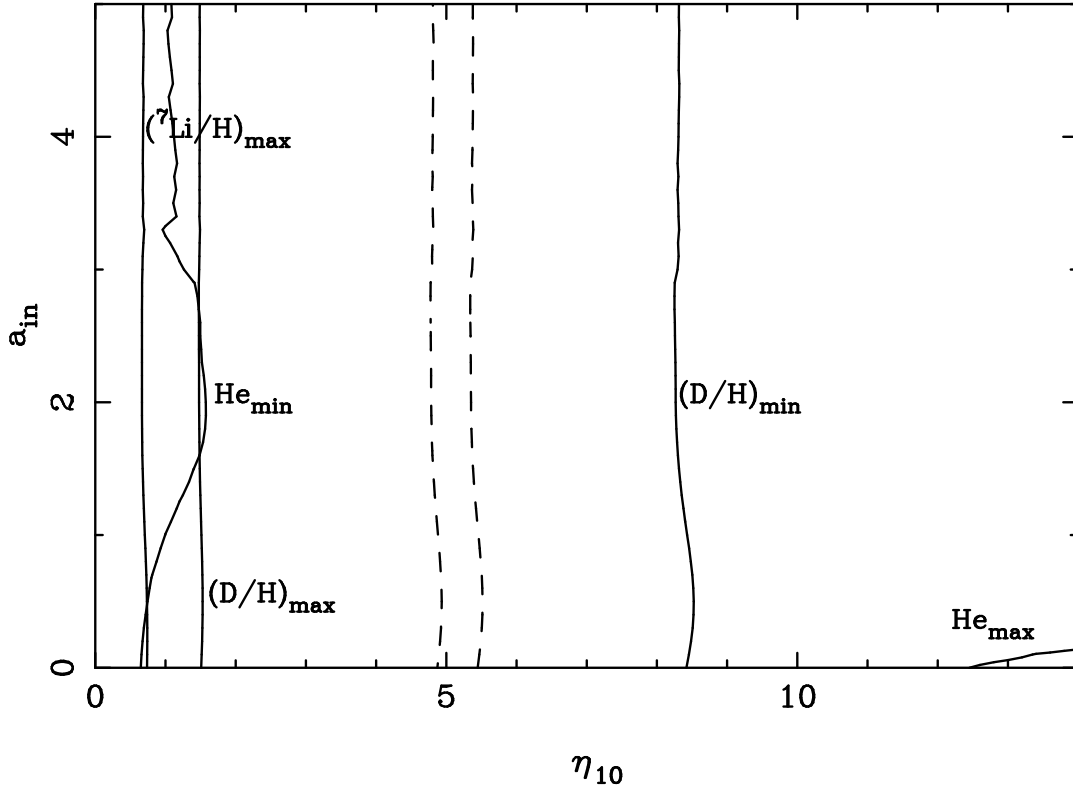


FIG. 3. Same as Fig. 2 for  $\beta = 40$ . The allowed region has now opened into a vertical strip essentially defined by the D/H lines. The wiggles in the  $\text{He}_{\text{min}}$  contour signal the presence of some numerical noise.



### Coupling function and $(n/p)$ ratios vs. temperature

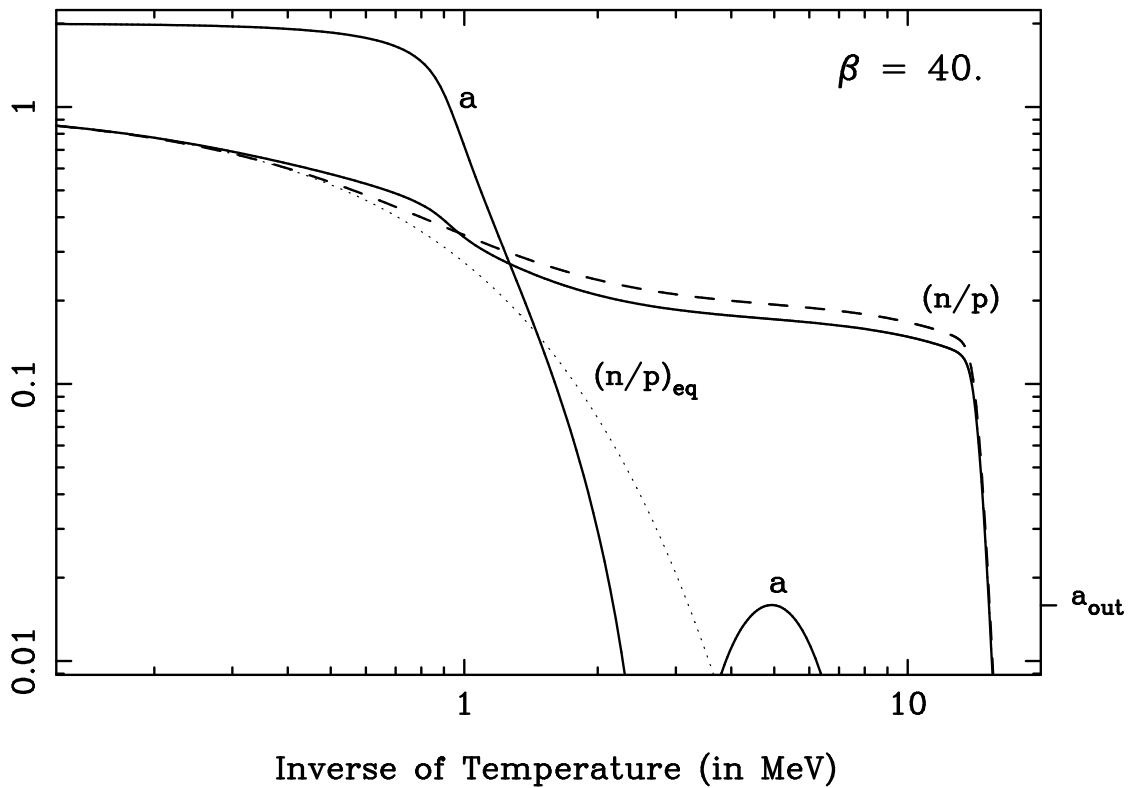


FIG. 4. Evolution of the coupling function  $a(\varphi)$ , and of the neutron to proton ratio, in function of the inverse of the physical temperature (for  $\beta = 40$  and  $a_{\text{in}} = 2$ ). The solid line is  $(n/p)$  in tensor-scalar gravity, the dashed line is  $(n/p)$  in general relativity, while the dotted line is the equilibrium value of the ratio  $(n/p)$ .  $a_{\text{out}}$  indicates the asymptotic level reached by  $a(\varphi)$  for small temperatures.

$a_{\text{out}}$  vs.  $a_{\text{in}}$  for  $\beta = 40$ .

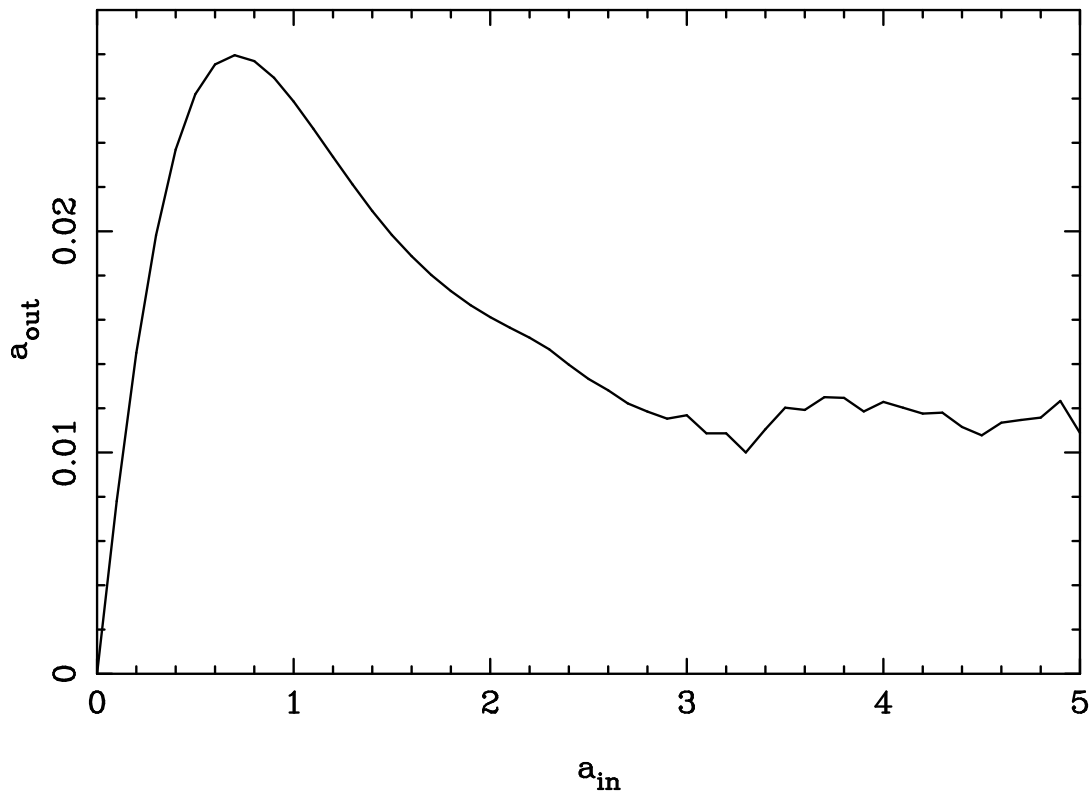


FIG. 5. Value of the final scalar coupling function  $a_{\text{out}} = a(\varphi_{\text{out}})$ , after BBN, in function of its initial value  $a_{\text{in}} = a(\varphi_{\text{in}})$  for  $\beta = 40$ . Because of the presence of a maximum in this curve the unlimited allowed region of Fig.3 still leads to a tight bound on  $a_{\text{out}}$ . The wiggles for  $a_{\text{in}} > 3$  are due to numerical noise.

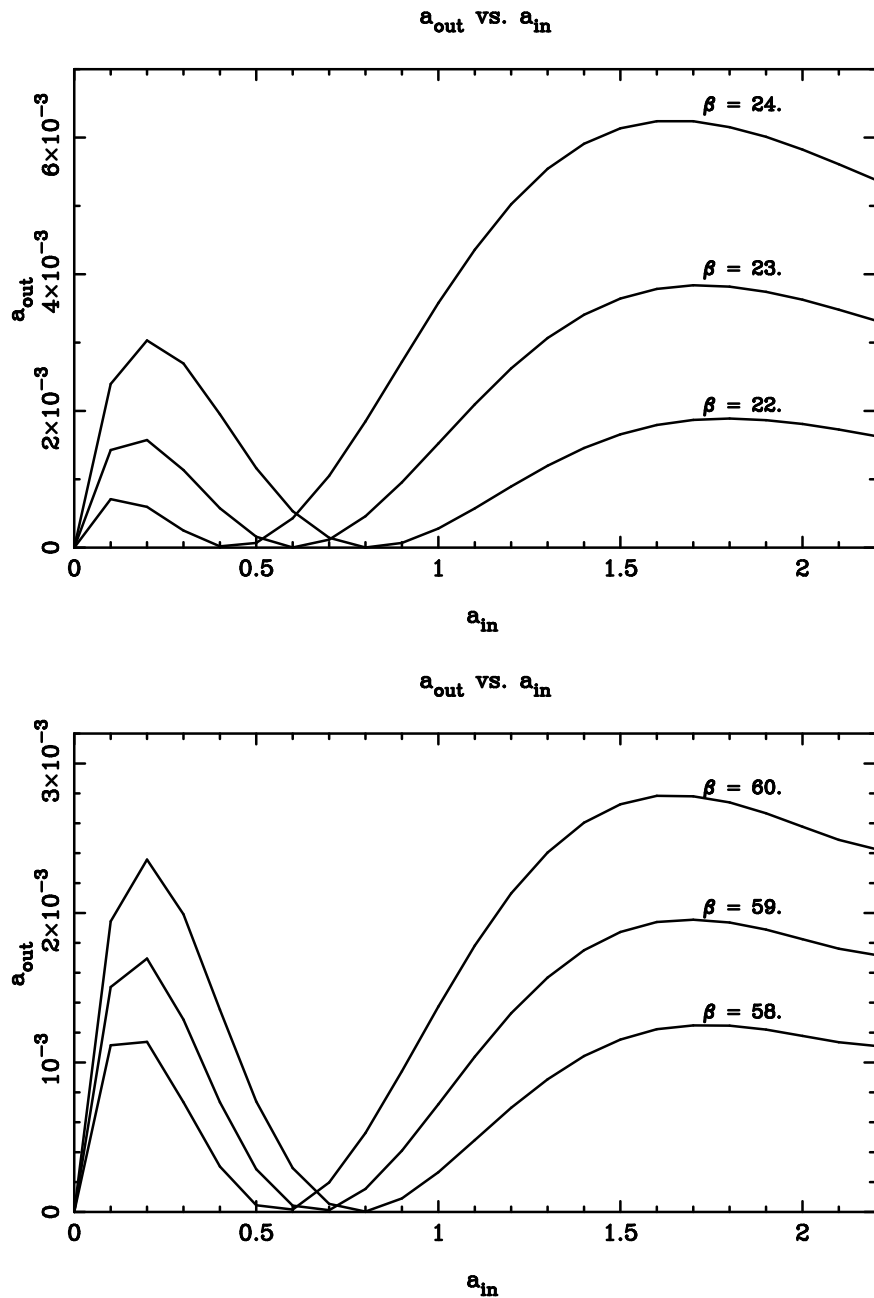


FIG. 6. Same as Fig. 5 for  $\beta = 22, 23$  and  $24$  (top panel), and for  $\beta = 58, 59$  and  $60$  (bottom panel). This figure illustrates the competition between two maxima in the curve  $a_{out}(a_{in})$ . For  $\beta \geq 23$  and  $\beta \geq 59$  it is the second maximum which determines the maximum allowed  $a_{out}$ .

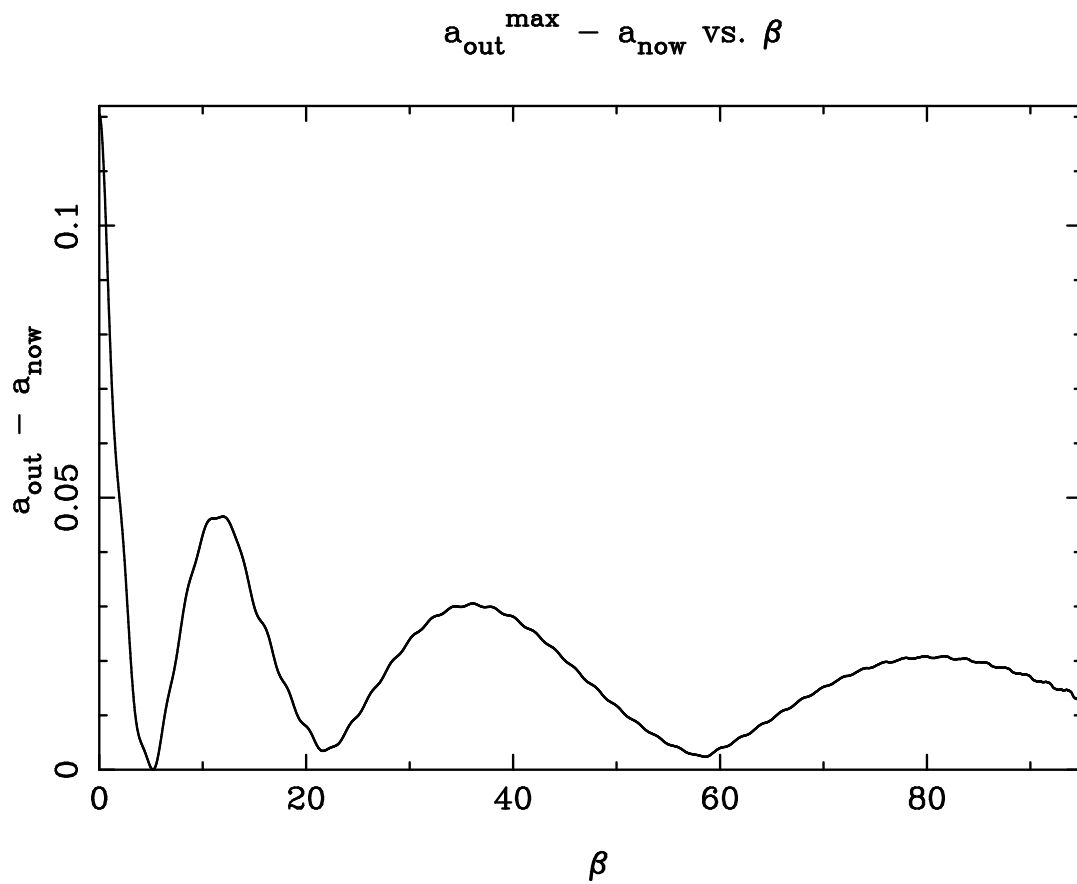


FIG. 7. Maximum BBN-allowed value of the difference  $a_{\text{out}} - a_0$  as a function of  $\beta$ .

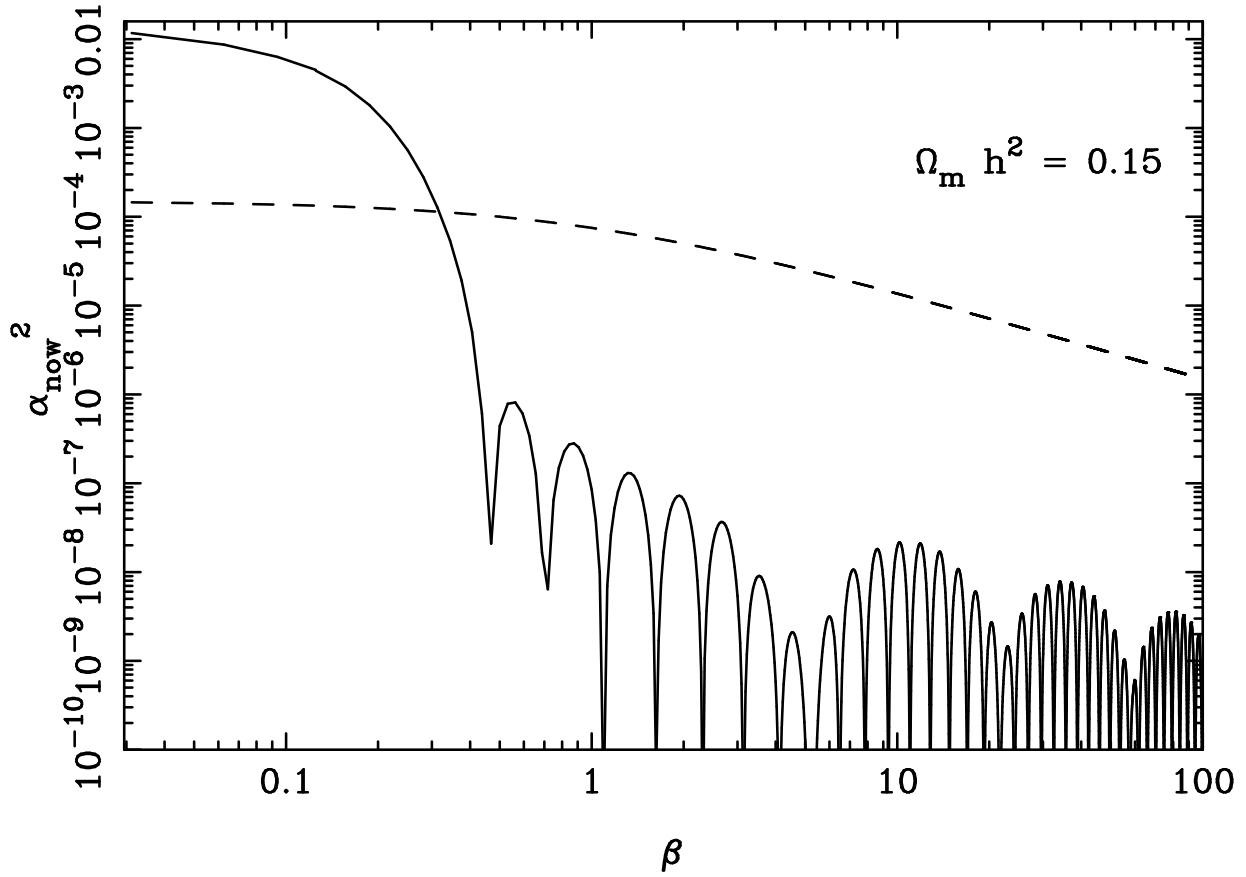


FIG. 8. The solid line represents the maximum BBN-allowed value of the present scalar-coupling parameter  $\alpha_0^2$  as a function of  $\beta$ . For comparison the dashed line represents the most stringent direct empirical bound on  $\alpha_0^2$ .

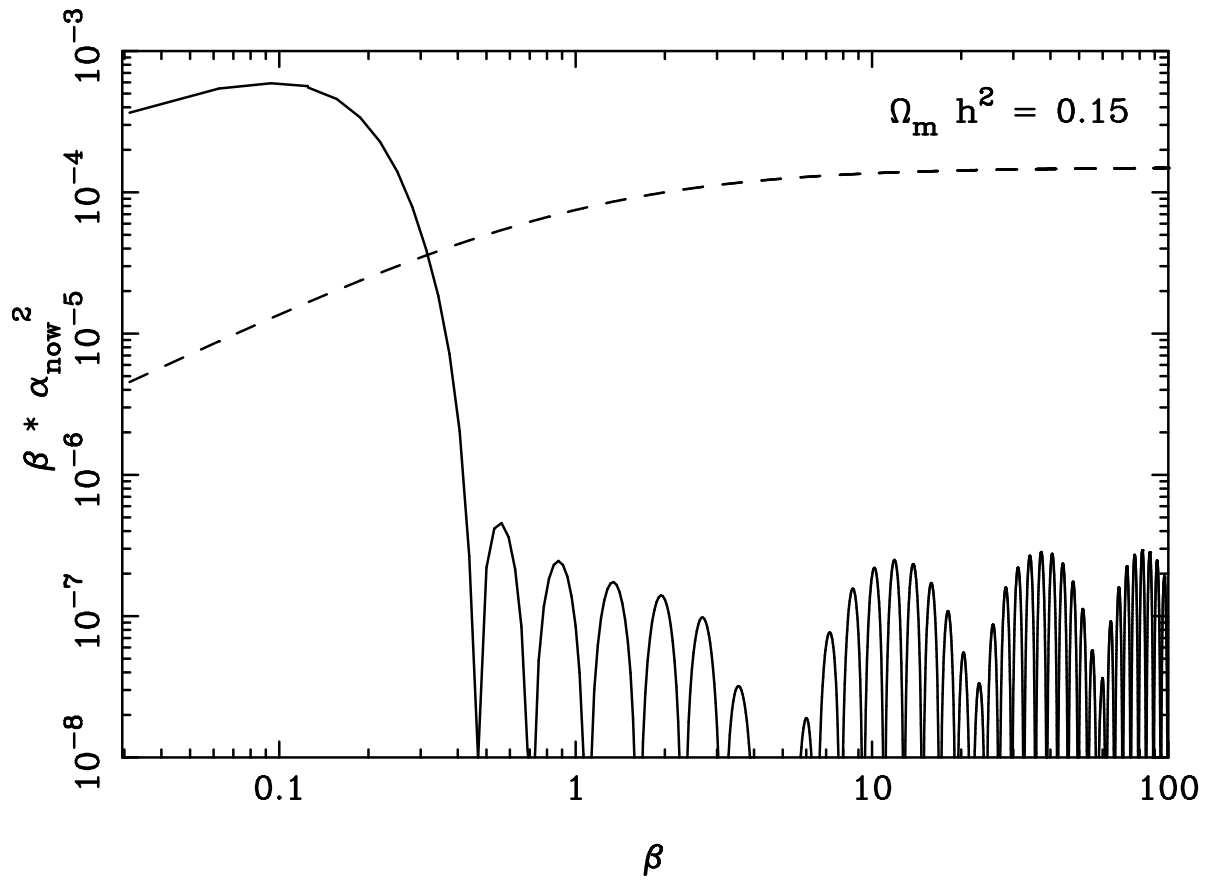


FIG. 9. Maximum BBN-allowed value of the product  $\beta \alpha_0^2$ . Lines as in Fig. 8.